ACS OMEGA

Open Access

http://pubs.acs.org/journal/acsodf

Article

Comprehensive Characterization of Some Selected Biomass for Bioenergy Production

Asmau M. Yahya, Adekunle A. Adeleke, Petrus Nzerem, Peter P. Ikubanni, Salihu Ayuba, Hauwa A. Rasheed, Abdullahi Gimba, Ikechukwu Okafor, Jude A. Okolie, and Prabhu Paramasivam*

Cite This: *ACS Omega* 2023, 8, 43771−43791

Read Online

ACCESS | Metrics & More | Article Recommendations

ABSTRACT: There is a lack of information about the detailed characterization of biomass of Nigerian origin. This study presents a comprehensive characterization of six biomass, groundnut shells, corncob, cashew leaves, *Ixora coccinea* (flame of the woods), sawdust, and lemongrass, to aid appropriate selection for bio-oil production. The proximate, ultimate, calorific value and compositional analyses were carried out following the American Standard for Testing and Materials (ASTM) standards. Fourier transform infrared spectroscopy, thermogravimetric analysis, scanning electron microscopy with energy-dispersive X-ray spectroscopy, and X-ray fluorescence were employed in this study for functional group analyses, thermal stability, and structural analyses. The H/C and O/C atomic ratios, fuel ratio, ignitability index, and combustibility index of the biomass samples were evaluated. Groundnut shells, cashew leaves, and lemongrass were identified as promising feedstocks for bio-oil production based on their calorific values (>20 MJ/kg). Sawdust exhibited favorable characteristics for bio-oil production as indicated by its higher volatile matter (79.28%), low ash content (1.53%), low moisture content (6.18%), and high fixed carbon content (13.01%). Also, all samples showed favorable ignition and flammability properties. The low nitrogen (<0.12%) and sulfur (<0.04%) contents in the samples make them environmentally benign fuels as a lower percentage of NO_x and SO_x will be released during the production of the bio-oil. These results are contributions to the advancement of a sustainable and efficient carbon-neutral energy mix, promoting biomass resource utilization for the generation of energy.

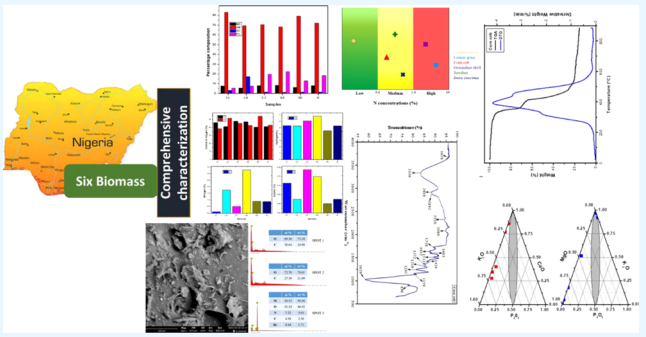

1. INTRODUCTION

The past few decades have seen significant growth in the global economy, driven by increasing population and urbanization.[1] The United Nations in 2017 projected the world's population to have reached 8.6 billion by 2030, and by 2050 and 2100 to be around 9.8 billion and 11.2 billion, respectively.[2] Inevitably, this will necessitate an increase in the energy demand in meeting the basic needs of society.[3] The modernization of the environment for life's convenience and activities would not have been actualizable without energy,[4] hence the exploration of various energy sources.[5,6] Fossil fuels account for 85% of the global energy demand. It was projected that by the year 2025, the demand would have grown by 50%.[7] Sokan-Adeaga and Ana[8] added that a major part of the increase would be coming from rapidly developing nations. Despite the many benefits of fossil fuels, their use has come under scrutiny due to their contribution to climate change through global warming.[9] The quantity of pollutants generated from the utilization of fossil fuels is the sequel to their usage on the high side.[10] With regard to the International Energy Agency report, global CO_2 emissions peaked at 36.3 billion tonnes in 2021.[11] This poses a grave risk to the environment as well as to public health. The United Nations has held numerous conferences and summits on climate change to address the issue of climate change mitigation. These gatherings have led to the formation of treaties and memorandums of understanding that outline the obligations of affiliate nations to decrease the release of greenhouse gases. One of the most significant outcomes of these conferences was the Paris Agreement, which resulted from COP21 in 2015.[12] The agreement provided a framework for reduction measures to climate change starting from 2020 and aimed at limiting global warming incidence to 1.5 °C, with a goal of attaining net-zero emissions by 2050. However, despite these efforts, the world still faces the challenge of decoupling economic growth from global warming. To reduce

Received: August 2, 2023
Revised: October 20, 2023
Accepted: October 26, 2023
Published: November 8, 2023

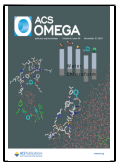

the effects of nonrenewable fuels on the environment, biomass utilization has been globally accepted as a renewable energy source.

As a result, the need to embrace the utilization of renewable energy sources as a great substitute for conventional fossil fuels for domestic and industrial applications has gained extraordinary attention.[9,13] Thus, it is essential to explore alternative and renewable energy sources to lessen the dependence on nonrenewable resources and serve as viable solutions to energy crisis.[10,14] Ahmed et al.[15] identified biomass, solar, wind, and tidal energies as the primary contributors to sustainable energy production. However, every energy source has its own pros and cons. Considering different renewable resources, the abundant nature of biomass has made it more attractive for its transformation into various products including biofuels, biobased materials, and chemicals using various processing technologies.[16] Similarly, biomass energy was said to offer a practical solution to various energy needs among renewable energy sources.[4] Biomass is the nonproduct output of agricultural production and processing that may contain materials that have some value for humans but whose cost of collection, transportation, and processing are greater than their economic value.[17] Biomass is the most copious source of energy on earth, including plants, animals, waste, and by-products of both plants and animals. Many countries are increasingly interested in the use of various biomass as raw materials to produce energy.[18] According to a report from IEA (2021),[19] biofuels provide approximately 3% of the world's fuel for transportation and are projected to meet 12% of worldwide transportation fuel demand by 2030. Previous studies revealed the conversion of biomass into gas or liquid fuels through various methods. In the realm of bioenergy and bio-oil production, there are two primary pathways: biochemical and thermochemical processes. The various biochemical processes are compositing, anaerobic digestion, and fermentation, while pyrolysis, carbonization, combustion, liquefaction, gasification, and supercritical oxidation are the various thermochemical processes of converting biomass into useful energy products.[20,21] Thermochemical treatment has gained prominence as an effective method for converting high-carbon parts into energy and/or fuel for reuse due to its ability to offer superior efficiency, economic performance, and volume reduction.[22] Among the thermochemical methods, pyrolysis, hydrothermal liquefaction, and supercritical water oxidation have been used to transform biomass into bio-oil. However, based on the highest fuel-to-feed ratios, pyrolysis is considered the most efficient technique.[23] Also, the most inexpensive and eco-friendly thermochemical conversion process of biomass to energy is pyrolysis.[24] Lyu et al.[25] noted that pyrolysis is a predominantly capable path for producing biofuels and other value-addition products. The liquid product obtained through pyrolysis (bio-oil or pyrolysis oil) has many unique features and potential applications. Bio-oil has the potential to substitute fuel oil, with a heating value equivalent to 40−50% of hydrocarbon fuels. Hu and Gholizadeh[26] also pointed out that bio-oil has various uses, such as low-grade fuel for boilers, high-grade fuel for car engines after upgrading, and so on. However, it is necessary to upgrade the bio-oil to be fully utilized as transport or engine fuel, which is both complicated and costly.[20] The developing nations are yet to fully enjoy the huge advantages that are enclosed in biomass as a source of energy.

For instance, Ezealigo et al.[27] stated that despite the huge potential of producing bioenergy from biomass in Nigeria, several challenges have hindered the actual production. One of these major setbacks is inadequate research and development in the country. It was suggested that there should be a reliable database for various potential feedstocks (biomass) in Nigeria for energy generation. However, a prerequisite to building such a database is a detailed characterization of various potential energy feedstock. Thus, the need to determine the properties of biomass for their effective utilization necessitated this work. The present study focused on six biomass (corncob, groundnut shell, cashew leaves, lemongrass, sawdust, and *Ixora coccinea*) in Nigeria, which were analyzed using various techniques such as proximate, ultimate, X-ray fluorescence, calorific value, scanning electron microscopy−energy-dispersive X-ray spectroscopy, Fourier transform infrared spectroscopy, and thermogravimetric analyses. The findings from these characterizations were analyzed with a view to providing the desired information on their potential for bio-oil production.

2. MATERIALS AND METHODS

2.1. Materials. In this study, six types of biomass were selected: corncob (CC), *I. coccinea* (IC) sawdust (SD), groundnut shell (GS), lemongrass (LG), and cashew leaves (CL). The corncob was collected from a farmland located in Utako, Abuja. The sawdust was collected from the wood workshop at the Nile University of Nigeria. Groundnut was purchased from a market in Karmo, Abuja, and the shells were obtained after removing the groundnut seed from the pod. *I. coccinea* was collected from a residence in Utako, Abuja. The cashew leaves were obtained from the premises of the university, and lemongrass was extracted from a field in Utako, Abuja. The samples were sun-dried to remove surface and residual moisture, pulverized, and then screened to 0.20 mm for characterization. Each sample was stored in a Ziploc bag and labeled accordingly.

2.2. Characterization of the Samples. *2.2.1. Proximate Analysis. 2.2.1.1. Moisture Content.* This was evaluated by following the ASTM E871−82[28] standard where the sample (0.5 g) was put into a preweighed ceramic crucible and placed in an oven (Uclear England, Model No: DHG-9053A) at a temperature of 105 °C before removal after 2 h. The samples were reweighed after cooling. Equation 1 was then employed to calculate the moisture content resulting from the mass loss after heating the air-dried samples.

$$\%\mathrm{MC} = \frac{W_S - (W_2 - W_1)}{W_S} \times 100 \quad (1)$$

where MC represents the sample's moisture content, W_S is the sample's air-dried weight, and W_1 and W_2 are the weights of the empty crucible and crucible with the sample after oven-drying, respectively.

2.2.1.2. Volatile Matter. To determine the volatile matter (VM), the ASTM E872−82[29] standard was adopted. The samples (2 g) were placed in crucibles and covered with ceramic lids before being placed in a muffle furnace (Vecstar Ltd., Mode/Serial No: LF3/F4244) at a temperature of 850 °C for 7 min. After, samples were cooled in a desiccator before reweighing the crucibles. The VM was evaluated using eq 2.

$$\%\mathrm{VM} = \frac{A - B}{A} \times 100 \quad (2)$$

https://doi.org/10.1021/acsomega.3c05656
ACS Omega 2023, 8, 43771−43791

where VM is the volatile matter of the sample, and A and B are the sample's initial and final weights, respectively.

2.2.1.3. Ash Content. Through the adoption of the ASTM E1755−01[30] standard, the ash content was determined. 2 g of samples were put into preweighed ceramic crucibles before subjecting it to a temperature of 730 °C for 5 h in a muffle furnace. The crucible lids were taken off before being placed in the furnace to ensure clean/complete combustion. The samples were cooled for an hour. The ash mass was then evaluated using eq 3.

$$\%\mathrm{AC} = \frac{W_2 - W_1}{W_S} \times 100 \tag{3}$$

where AC is the ash content of the sample, W_1 and W_2 represent the weights of the empty crucible and crucible with the ash, respectively, and W_S is the weight of the sample.

2.2.1.4. Fixed Carbon. The amount of fixed carbon was estimated by difference, where all other constituents (MC, VM, and AC) were subtracted as percentages from 100 using eq 4.

$$\%\mathrm{FC} = 100 - (\%\mathrm{VM} + \%\mathrm{AC} + \%\mathrm{MC}) \tag{4}$$

For data reliability and reproducibility, the proximate analysis was performed in triplicate.

2.2.2. Ultimate Analysis. A representative sample weighing 2 g was placed in a crucible. The carbon, hydrogen, and nitrogen contents were determined by utilizing LECO−CHN628 Analyzer (Model No: 622−000−000, SN-12357) following the ASTM D5373−16 standard.[31] The sulfur content was determined by employing LECO S-144DR Sulfur Determinator (Model No: 606−0000−300, SN-477) in line with the ASTM D4239−11 standard.[32] Equation 5 was employed in determining the oxygen content.

$$\%\mathrm{O} = 100 - (\%\mathrm{C} + \%\mathrm{H} + \%\mathrm{N} + \%\mathrm{S} + \mathrm{ash}) \tag{5}$$

2.2.3. Fourier Transform Infrared (FTIR) Spectroscopy. The Shimadzu Fourier Transform Infrared (FTIR) spectrophotometer (Model no: 8400S) was utilized in identifying and measuring the chemical compounds present in the samples based on their infrared radiation absorption within the scanning absorption range of 600−4000 cm^{-1} at a resolution of 4 cm^{-1}.

2.2.4. Scanning Electron Microscopy−Energy-Dispersive X-ray Spectroscopy (SEM-EDS). The SEM-EDS Phenom ProX model was used in the examination of the morphology of the biomass samples. The images were captured from the SEM after which they were saved, and the energy-dispersive X-ray (EDX) revealed the elements present with the molar concentration in percentage.

2.2.5. Thermogravimetric Analysis (TGA). The PerkinElmer TGA 4000 was used with a test sample of about 6.5 mg placed into the crucible. The experimental procedure was conducted in an inert environment with a constant flow of nitrogen gas at a rate of 100 mL/min. The samples were heated at a rate of 15 °C/min between 20 and 800 °C. The thermogravimetric data collected were compiled into a plot known as a TGA curve. For differential thermal analysis, the derivative thermogravimetric (DTG) curve obtained from the first derivative of the TGA curve was also plotted. Thermal parameters such as $T_{burnout}$, T_{offset}, DTG_{peak}, T_{peak}, and T_{onset} were also obtained from the TGA measurements.

2.2.6. Calorific Value. The higher heating value (HHV) of the samples was determined using the Bomb Calorimeter (Model 6100, Bomb Calorimeter, Parr Instrument Co., Moline, Illinois) following the ASTM D5865−04 standard.[33]

2.2.7. X-ray Fluorescence (XRF). In this study, the X-ray fluorescent Nitron 3000 was utilized and left to stabilize for 5 min after initialization. The Cu−Zn method was selected for this analysis, as it can detect high levels of elements and sesquioxide due to its high intensity. The sample was set on the sample holder, the ray point was directed over it, and data collection was initiated. Data were collected in triplicate, and the average was calculated automatically. Using this data, calculations for slagging and fouling indices were made using eqs 6−8.

$$\frac{\mathrm{S}}{\mathrm{A}} = \frac{\%[\mathrm{SiO_2}]}{\%[\mathrm{Al_2O_3}]} \tag{6}$$

$$\frac{\mathrm{I}}{\mathrm{C}} = \frac{\%[\mathrm{Fe_2O_3}]}{\%[\mathrm{CaO}]} \tag{7}$$

$$S_r = \frac{\%[\mathrm{SiO_2}]}{\%[\mathrm{SiO_2} + \mathrm{Fe_2O_3} + \mathrm{CaO} + \mathrm{MgO}]} \times 100 \tag{8}$$

where S/A is the silica/alumina ratio, I/C is the iron/calcium ratio, and S_r is the slagging viscosity index.

2.3. Fuel Ratio, Ignitability Index, and Combustibility Index. The fuel ratio, ignitability, and combustibility indices of the biomass samples were evaluated using eqs 9, 10, and 11, respectively.

$$\mathrm{FR} = \frac{\mathrm{FC}}{\mathrm{VM}} \tag{9}$$

$$I_I = \frac{\mathrm{CV} - 81\mathrm{FC}}{\mathrm{VM} + \mathrm{MC}} \tag{10}$$

$$\mathrm{CI} = \frac{\mathrm{CV}}{\mathrm{FR}} \times (115 - \mathrm{ash}) \times \frac{1}{105} \tag{11}$$

where FR is the fuel ratio, FC is the fixed carbon, VM is the volatile matter, CV is the calorific value, I_I is the ignitability index, CI is the combustibility index, and MC is the moisture content.

2.4. H/C and O/C Atomic Ratios. The H/C and O/C atomic ratios were determined by using eqs 12 and 13, respectively.

$$\mathrm{H{:}\ C\ ratio} = \frac{\%\text{hydrogen content}}{\%\text{carbon content}} \tag{12}$$

$$\mathrm{O{:}\ C\ ratio} = \frac{\%\text{oxygen content}}{\%\text{carbon content}} \tag{13}$$

2.5. Compositional Analyses. *2.5.1. Extractives Content.* 2.5 g of sample and 150 mL of acetone were put into a cellulose thimble of a Soxhlet extractor with acetone serving as the solvent for the extraction. Carefully regulated residence time (25 min) and temperature (70 °C) for the boiling and rising stages were utilized in heating the sample for a 4 h run. Following this process, at room temperature, the sample was air-dried for 5 min. At 105 °C, the sample was oven-dried to achieve a constant weight. Using eq 14, the evaluation of the extractives' weight (%w/w) was done.

$$\text{extractives} = A - B \tag{14}$$

https://doi.org/10.1021/acsomega.3c05656
ACS Omega 2023, 8, 43771−43791

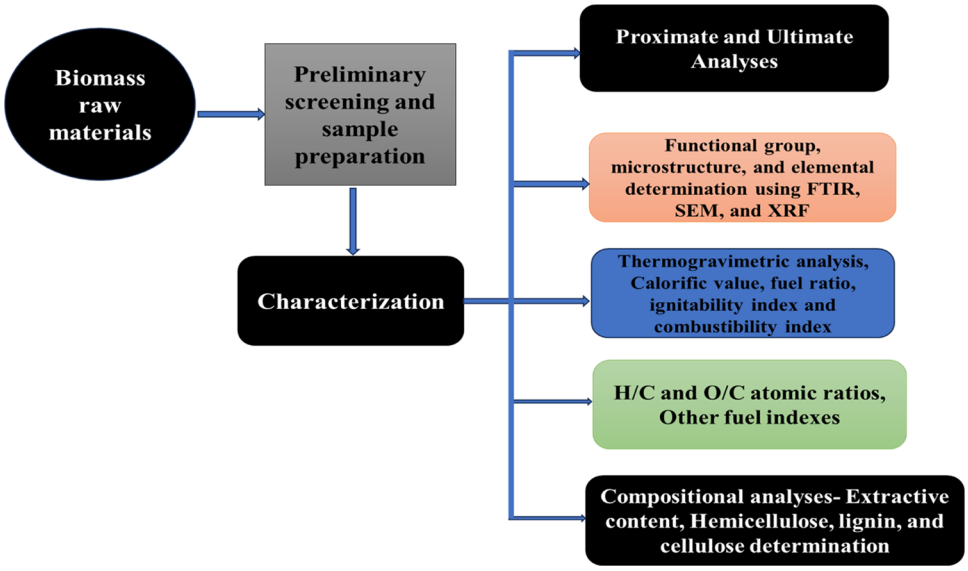

Figure 1. Overview of the methodology used.

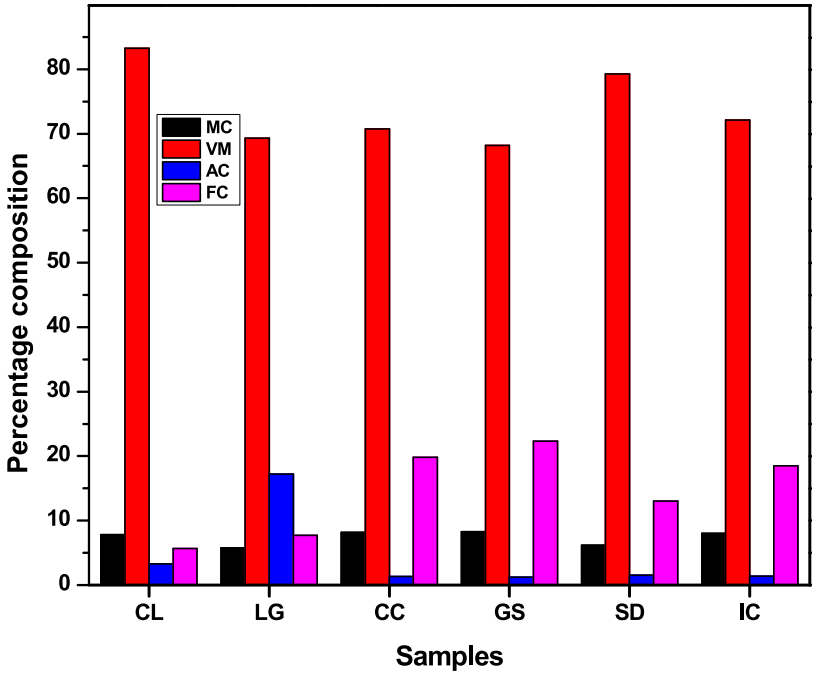

Figure 2. Proximate analysis of biomass samples.

where A and B are the weights of extractive-laden and extractive-free samples, respectively.

2.5.2. Hemicellulose Determination. Extractive-free sample (1 g) was put into a 250 mL Erlenmeyer flask in which 150 mL of a 0.500 mol/dm^3 NaOH concentration was added. Boiling of the mixture using distilled water was done for 3 and a 1/2 h. Subsequently, the solution was cooled and filtered via vacuum filtration and then washed to achieve a neutral pH. After, the filtrate was dried at 105 °C to achieve a constant weight in an oven. The hemicellulose content of the sample (%w/w) was then evaluated by subtracting the difference between the weight of the sample prior to and following this treatment as shown in eq 15.

$$\text{hemicellulose} = C - D \tag{15}$$

where C and D are the weights of extractive-free sample and the weight after heating, respectively.

2.5.3. Lignin Determination. 0.3 g of extractive-free sample was measured and placed into a glass test tube. Next, 3 mL of 72% H_2SO_4 was added and the sample was left at room temperature for 2 h. The mixture was carefully shaken every 30 min to ensure complete hydrolysis. When the initial hydrolysis was complete, distilled water (84 mL) was added, and an autoclave was used to conduct the second hydrolysis at 121 °C for 1 h. The obtained slurry was cooled before it was vacuum-filtered via a filtering crucible. To determine the quantity of acid-insoluble lignin present, the residues were dried at 105 °C while the weight changed. Meanwhile, a UV−vis spectrophotometer was used to determine the acid-soluble lignin fraction. This was achievable through the measurement of the

https://doi.org/10.1021/acsomega.3c05656
ACS Omega 2023, 8, 43771−43791

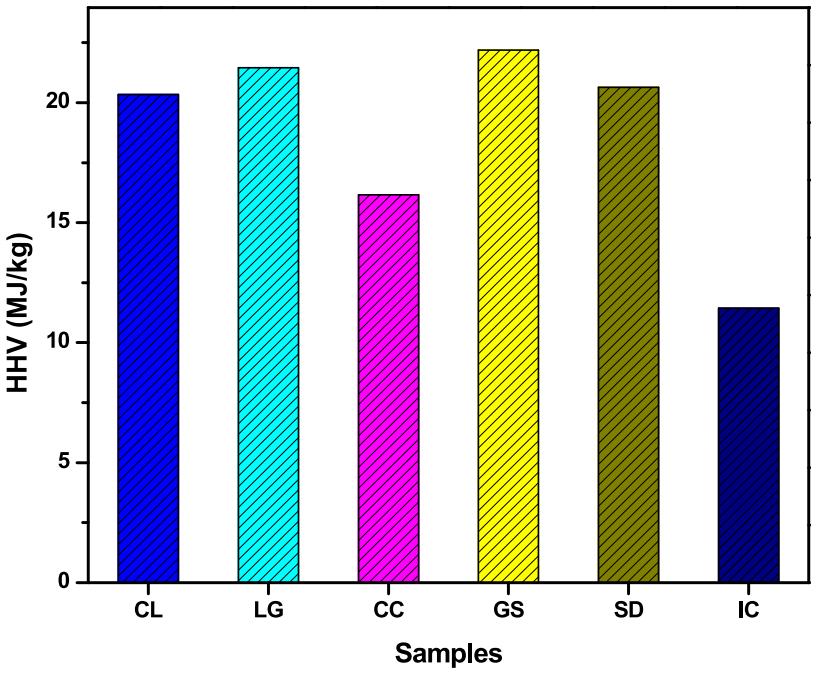

Figure 3. Higher heating value of samples.

absorbance of the acid-hydrolyzed samples at 320 nm. Finally, the total lignin content was calculated by summing up the fractions of the acid-soluble and acid-insoluble lignin.

2.5.4. Cellulose Determination. The cellulose content (% w/w) was estimated using eq 16 by assuming that the constituents present in biomass materials are extractives, cellulose, hemicellulose, lignin, and ash.

$$\text{cellulose} = 100\% - (\text{hemicellulose} + \text{lignin} + \text{ash} + \text{extractives}) \quad (16)$$

2.6. Other Fuel Indexes. Fuel indexes such as molar Si/K ratio as a pointer for K release, molar 2S/Cl ratio as a pointer for high-temperature corrosion risks, and molar (Si + P + K)/(Ca + Mg) for ash-melting problems were evaluated.

Figure 1 gives a comprehensive illustrative methodology used in this study.

3. RESULTS AND DISCUSSION

3.1. Proximate, HHV, and Ultimate Analyses. The proximate values of the samples used for the study are listed in Figure 2. Volatile matter (VM) represents the quantity of condensable and noncondensable vapors that are released during the combustion of the fuel[10,34] at a heating temperature of 400 and 500 °C.[35] Figure 2 reveals that cashew leaves exhibited the highest VM content (83.24%), while groundnut shell had the lowest (68.17%). It can be observed that the VM content of cashew leaves in this study was significantly greater than the value of 65.33% reported by Bhavsar et al.[36] Conversely, the VM content of groundnut shell in our study was lower compared with the results of 76.90%,[37] 75.27,[38] 80.24,[39] and 75.57%[40] but slightly higher than 64.63%.[41] These variations can be attributed to geographical differences. However, the VM obtained for corncob (70.72%) and sawdust (79.28%) align with the findings of Liu et al.[42] (69.5%) and Varma et al.[43] (80.87%). The VM content of lemongrass (69.32%) obtained in this current study was higher than the 59.99% attained by Madhu et al.[44]

Biomass materials typically exhibit high VM content due to their organic nature, indicating their potential to generate significant inorganic vapors quantities amounts of inorganic vapors during utilization as feedstock.[45] Biomass generally has up to 2.5 times more VM than coal.[46] A high percentage of VM indicates that a substantial portion of the fuel is burnt as gas resulting in rapid and challenging combustion as well as smoke formation.[10] Moreover, high VM makes biomass hydrophilic.[47] While an increase in VM enhances ignition characteristics, excessively high VM content can lead to combustion performance degradation owing to an increase in flue gas volume generated by VM.[48] It has been highlighted that fuels with higher VM content necessitate a larger quantity of high-pressure secondary air to achieve efficient combustion.[49] However, incomplete combustion of the VM can give rise to undesirable outcomes, such as the emission of dark smoke, heat loss, environmental pollution, and the deposition of soot on boiler surfaces.

Fixed carbon (FC) is the carbonaceous material that remains after the devolatilization of biomass.[34,50] Generally, biomass is known to have lower fixed carbon content.[47] In this study, the FC content of the biomass samples decreased in the order of groundnut shell (22.34%) > corncob (19.81%) > *I. coccinea* (18.50%) > sawdust (13.01%) > lemongrass (7.69%) > cashew leaves (5.69%). The FC content for corncob is in trend with the findings of Onokwai et al.,[10] Akogun and Waheed,[51] Anukam et al.,[45] and Ibeto et al.[18] For sawdust, the FC contents reported by Varma et al.[43] and Mensah et al.[52] were 12.68 and 13.33 ± 0.8%, respectively, which tallies with the result obtained in this study (13.01%). However, previous studies reported higher FC percentages for lemongrass (24.78%)[44] and cashew leaves (16.87%).[36] The FC content of groundnut shell (22.34%) finds agreement with the value (22.28%) obtained by refs 53[54]. However, no FC was recorded in ref. 55 This disparity highlights the variations in biomass

https://doi.org/10.1021/acsomega.3c05656
ACS Omega 2023, 8, 43771−43791

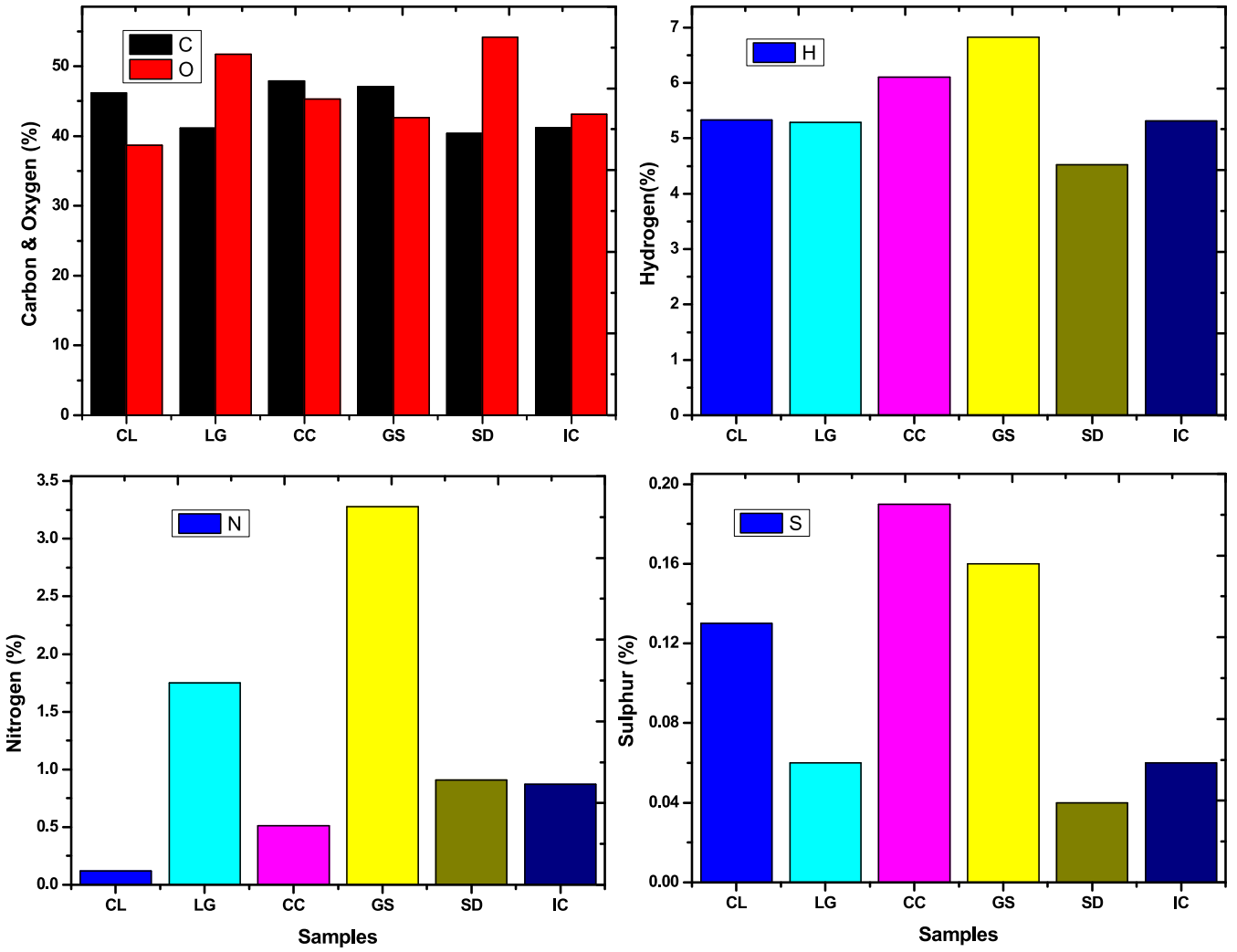

Figure 4. CHNSO compositions of the samples.

samples, influenced by factors including soil type and geographical location. The effect of FC on biomass is usually reflected in its HHV (Figure 3) as there exists a very strong relationship between the parameters.

The biomass investigated had low ash content (AC) except for lemongrass which had an AC of 17.2%. This was higher than the 7.02% reported for lemongrass by Madhu et al.[44] The ACs in the present study for corncob (1.32%), groundnut shell (1.21%), and sawdust (1.53%) were comparable with the findings of 1.05,[56,57] 1.3,[58] and 1.13%,[52] respectively. Biomass ash consists primarily of oxide forms of silica, aluminum, titanium, potassium, iron, magnesium, and sodium.[59] Unlike coal combustion residues, biomass ashes tend to have higher contents of CaO, SO_3, and Cl, while exhibiting lower levels of Al_2O_3, SiO_2, and Fe_2O_3[46,60] High AC can adversely affect the efficiency of thermochemical conversions, leading to issues such as fouling, slagging, and corrosion in equipment.[57,61,62] Moreover, a higher concentration of ash in the biomass material during the process of combustion or pyrolysis acts as a heat sink, thereby reducing the combustion system's efficiency.[63] He et al.[64] emphasized the suitability of feedstock with low AC for fuel production, while materials with high AC are better suited for use as fertilizers. Hence, the high AC of lemongrass observed in this study makes it a potential material for fertilizer production.

Moisture plays a crucial role in biomass utilization, influencing its behavior during pyrolysis and impacting the quality of the resulting pyrolysis liquid.[65] Notably, qualitative observations have shown that dry feed materials tend to produce highly viscous oil.[65]

High MC in biomass can pose logistical challenges as it increases the tendency for decomposition, resulting in energy loss, and impacting cost and energy balances.[66] For combustion, low MC in biomass is desirable, as high MC presents challenges during burning. In this study, the MC of the biomass ranged from 5.79 to 8.28%, which falls below the recommended limit of 10−12% set by Austria and German standards for fuel pellets and briquettes.[67] Having a low MC enhances the ignition ability of biomass, with improved combustion quality and a reduction in the release of objectionable smoke and toxic gases.[68]

With regard to bio-oil production, biomass having a higher VM, low AC, low MC, and high FC is deemed more suitable. The availability of significant quantities of volatile material enhances volatility as well as reactivity, favoring bio-oil production.[69] Studies conducted on different biomass revealed that biomass with higher AC resulted in lower bio-oil and higher biochar yields[70] and vice versa.[10,71−73] The low MC observed in the samples makes them well suited for the pyrolysis process. This characteristic is advantageous as it

https://doi.org/10.1021/acsomega.3c05656
ACS Omega 2023, 8, 43771−43791

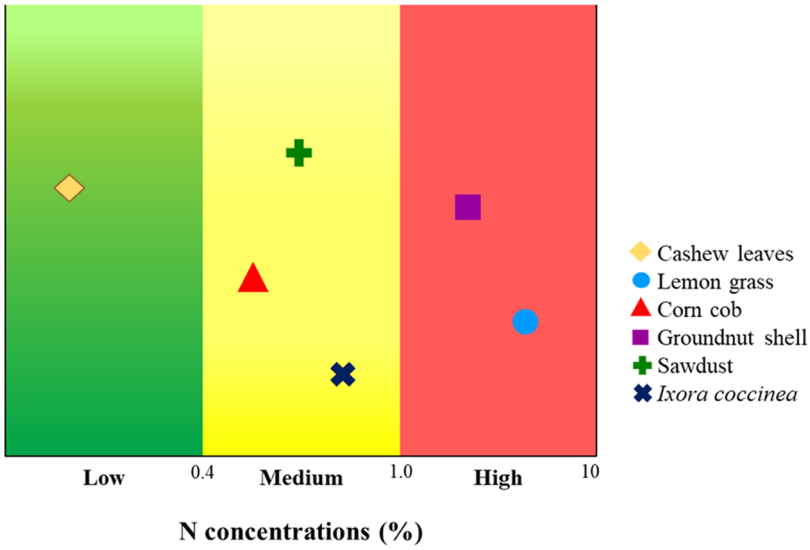

Figure 5. Classification of biomass based on nitrogen concentration.

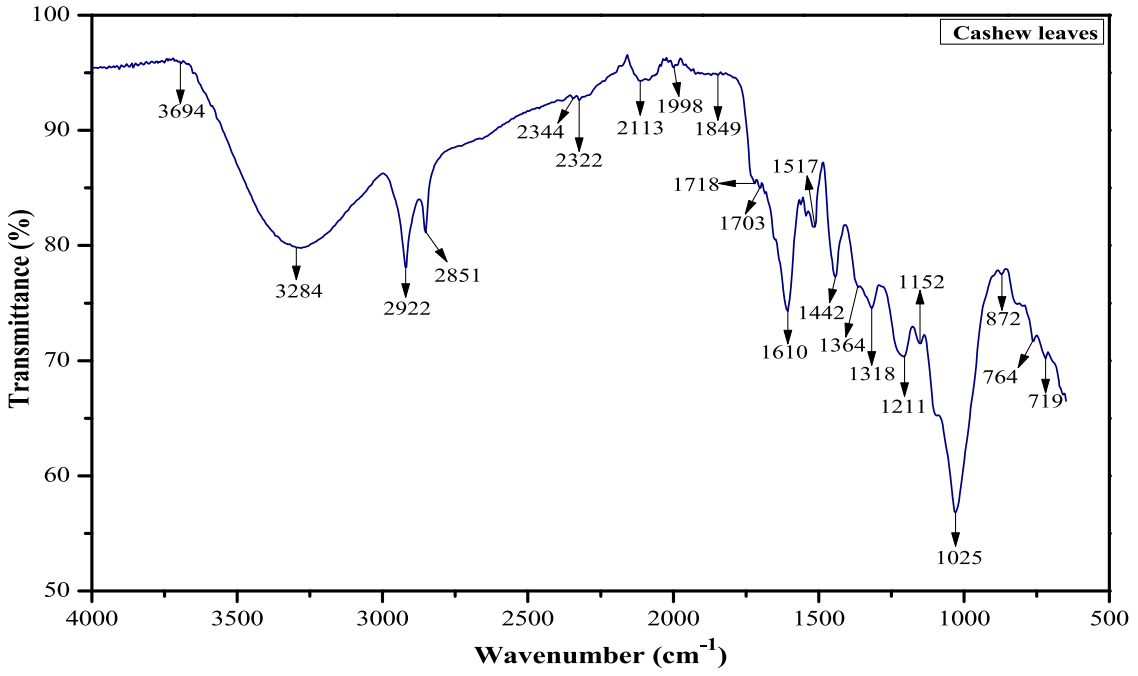

Figure 6. FTIR spectrum of cashew leaves.

requires less energy to vaporize the biomass in the reactor, thereby enhancing the generation of thermal energy and conversion efficiency during pyrolysis.[10] Also, high FC enhances the time to yield bio-oil as it releases a significant amount of energy.[10]

All biomass had significant calorific values ranging from 11.4346 to 22.1848 MJ/kg, showing their potential as energy sources. Groundnut shell had the highest HHV (Figure 3), which can be linked to its higher FC content.[74] The reported HHV of corncob (16.16 MJ/kg) in various literature falls within the range of 16.15−19.28 MJ/kg,[10,45,51,58,75−77] which aligns with the finding of this study (16.16 MJ/kg). Similarly, the HHV of sawdust obtained in this study (20.64 MJ/kg) falls within the range of 11.29−26.10 MJ/kg.[78] The HHV (22.18 MJ/kg) of groundnut shells obtained in the present study exceeds values obtained by other researchers: 15.68,[79] 18.32,[37] 18.64,[39] 15.69 ± 0.10,[40] and 17.69 MJ/kg.[54]

HHV is also associated with moisture content in that it poses challenges during combustion by reducing energy efficiency and heating value. This diminishes its usefulness as a fuel source. Consequently, high MC leads to a decrease in HHV.[80] It was revealed that lemongrass, sawdust, and cashew leaves had the lowest MC and hence a high HHV. High VM does not translate to a high HHV, as some components of VM are derived from noncombustible gases.[81] The influence of ash extends beyond its inert effect on the HHV as it also hampers the apparent heat obtained from the combustion of biomass.[81,82]

The elemental constituents of the biomass samples perform specific functions in the determination of biomass fuel efficiency and potential pollutant behavior.[83] The ultimate

https://doi.org/10.1021/acsomega.3c05656
ACS Omega 2023, 8, 43771−43791

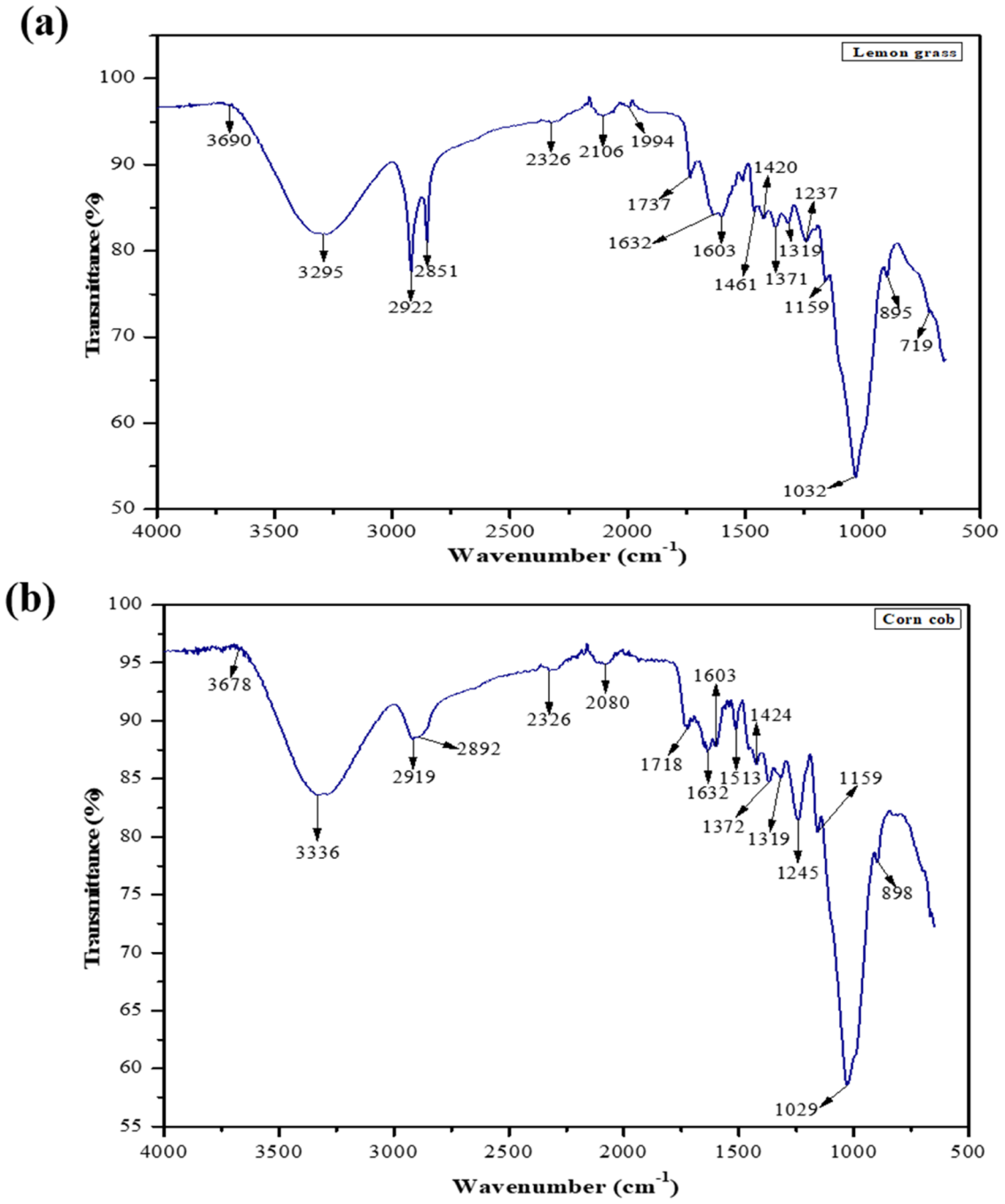

Figure 7. FTIR spectra of (a) lemongrass and (b) corncob.

analysis results (Figure 4) reveal the compositions of each element in the biomass samples. The carbon content in the investigated corncob samples aligns with the range of 47−49% reported by Trninić et al.[84] and Demiral et al.[77] and corn stover reported by Capunitan and Capareda.[85]

Through thermochemical conversion technologies, the HHV and FC contents are increased by carbon content.[86] Hydrogen content also contributes to increase the HHV value while nitrogen has the opposite effect.[80] The oxygen content is the most vital fuel property because it gives the combustion behavior of the fuel. During the thermochemical conversion processes (pyrolysis), thermal reactivity is increased due to higher oxygen content.[87] Nitrogen and oxygen contents are indicative of potential gas emissions during combustion. Inna et al.[80] noted that NO_2 is a hazardous respiratory toxic and when combined with sunlight contributes to ozone depletion. Biomass fuels can be classified based on nitrogen concentrations (Figure 5) as low-N fuels (<0.4%), medium-N fuels (0.4−1%), and high-N fuels (1−10%).[88]

According to Oluwatosin et al.,[89] biomass with nitrogen <2.0% and sulfur <0.2% is desirable as a fossil fuel substitute due to the lower risk of emitting toxic oxides during pyrolysis or combustion. All samples investigated fall within this desirable range, except for the groundnut shell, which had a nitrogen content of 3.28%.

According to Sulaiman et al.,[90] a biomass is adjudged good when it has a carbon content of 47−54%, hydrogen content of 5.6−7%, oxygen content of 40−44%, nitrogen content of 0.1−

https://doi.org/10.1021/acsomega.3c05656
ACS Omega 2023, 8, 43771−43791

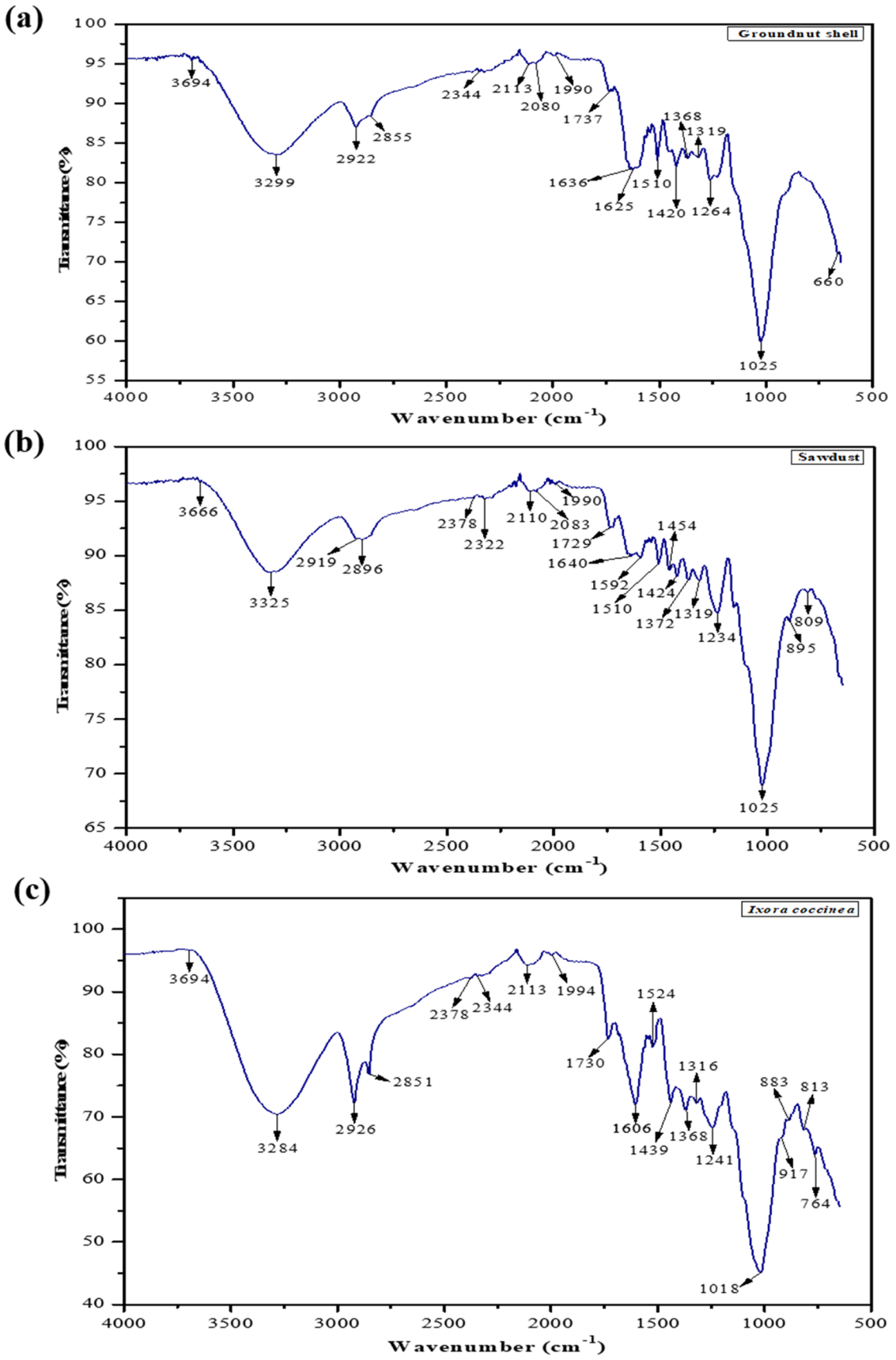

Figure 8. FTIR spectra of (a) groundnut shell, (b) sawdust, and (c) *I. coccinea*.

0.5%, and sulfur content around 0.1%. Hence, cashew leaves and corn cobs are potential candidates for bio-oil production.

3.2. Fourier Transform Infrared (FTIR) Spectroscopy.

The obtained FTIR spectra (Figures 6, 7, and 8) revealed

https://doi.org/10.1021/acsomega.3c05656
ACS Omega 2023, 8, 43771−43791

Table 1. Functional Groups of the Peaks Observed in the Samples[a]

functional groups/band assignments	CL	LG	CC	GS	SD	IC
−OH stretch	3694, 3284	3295	3678, 3336	3694, 3299	3666, 3325	3694, 3284
aliphatic (methylene) C−H asymmetric stretch	2922	2922	2919	2922	2919	2926
aliphatic (methyne) C−H asymmetric stretch	X	X	2892	X	2896	X
aliphatic (methylene) C−H symmetric stretch	2851	2851	X	2855	X	2851
O═C═O (carbon dioxide)	2344, 2322	X	2326	2344	2378, 2322	2378, 2344
C≡C terminal alkyne (monosubstituted)	2113	2106	X	2113	2110	2113
transition metal carbonyl	X	X	2080	2080	2083	X
N═C═S (isothiocyanate)	1998	X	X	1990	1990	1994
five-membered ring anhydride (carbonyl)	1849	X	X	X	X	X
C═O ester fatty acid (carbonyl)	1718	1733	1718	1737	1729	1730
carboxylic acid (carbonyl)	1703	X	X	X	X	X
alkenyl C═C stretch	X	X	1632	X	1640	X
aryl-substituted C═C	X	X	X	1625	X	X
C═C−C aromatic ring stretch	1610	1603	1603	X	1592	1606
	1517	X	1513	X	X	1524
C═C−C aromatic ring stretch	X	1510	X	1510	1510	X

[a]X − Unavailable data.

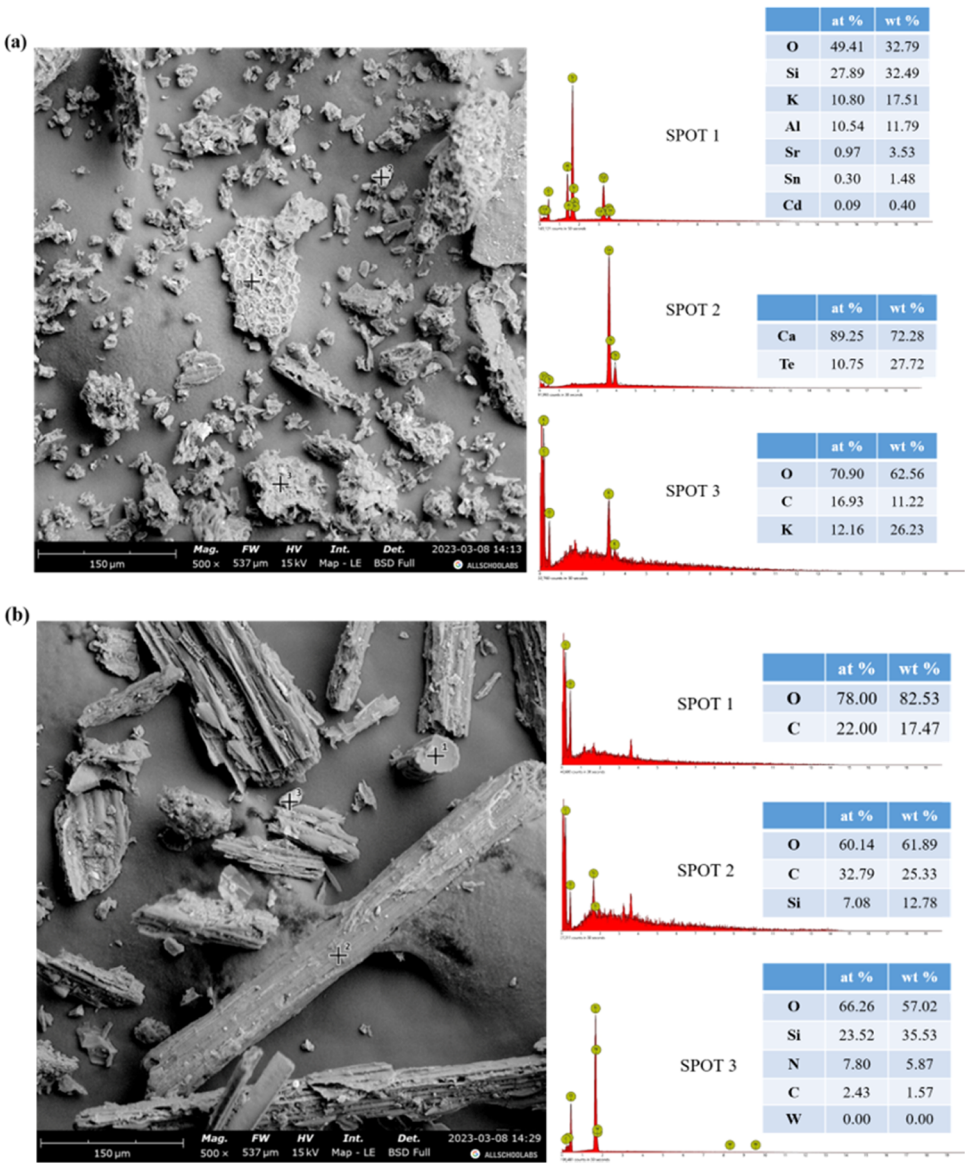

Figure 9. Micrographs and elemental composition of (a) cashew leaves and (b) lemongrass leaves.

https://doi.org/10.1021/acsomega.3c05656
ACS Omega 2023, 8, 43771−43791

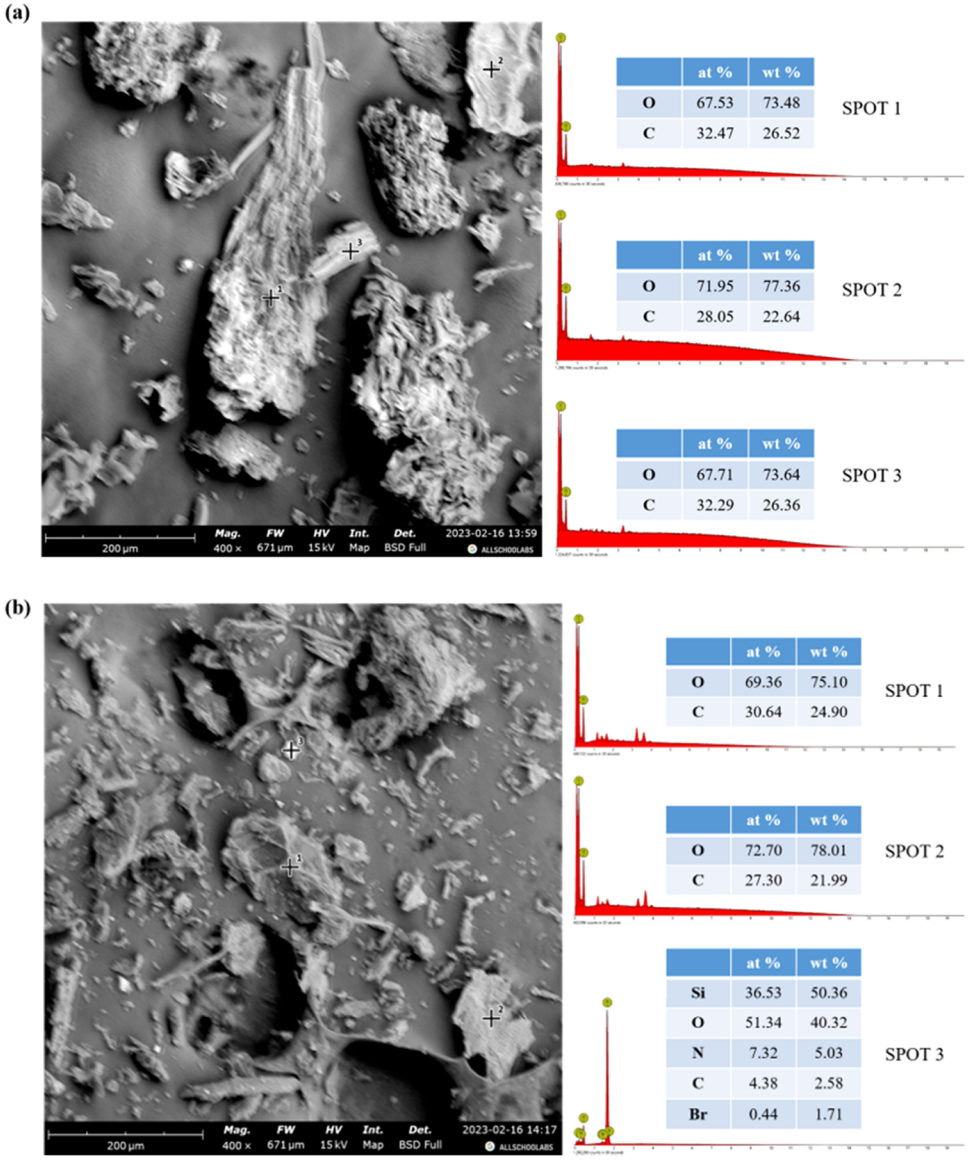

Figure 10. Micrographs and elemental composition of (a) corncob and (b) groundnut shell.

characteristic peaks present in the samples. All samples exhibited multiple peaks (>5) in their spectra, indicating their complex nature. The spectra showed similarity in peak patterns which indicate the existence of similar functional groups across the biomass materials. Table 1 gives a summary of the identified functional groups. Generally, raw biomass is composed of alkenes, aromatics, ketones, esters, and alcohols, with different oxygen-based functional groups such as OH at 3400−3200 cm^{-1}, C═O at 1765−1715 cm^{-1}, and C−O−C at 1270 cm^{-1}.[91] However, sawdust and corncob showed distinct peaks at 2896 and 2892 cm^{-1}, signifying the presence of an aliphatic (methyne) C−H asymmetric stretch group.

The spectra of all samples revealed peaks in the broadband between 3340 and 3200 cm^{-1} region, and this corresponds to the hydroxyl group (−OH). This is an indication of the existence of bonds to form moisture. This is most probably attributed to the presence and interaction of various derivatives of alcohol, phenol, amino, and carboxyl groups.[92] Similar findings have been reported by some researchers,[93,94] who identified the band at 3600−3200 cm^{-1} as representing the hydrogen-bonded −OH groups stretching vibration of phenolic and aliphatic structures. Similar peaks depicting OH associations were observed at 1470−1420 cm^{-1} in the samples.[95,96] The presence of peaks corresponding to C═C aromatic rings in the biomass samples indicates the presence of lignin.[96] These aromatic double bonds impart properties such as increased stabilization, conjugation, and rigidity. The low transmittance of the signal in the range of 1032−1025 cm^{-1} implies the occurrence of cellulose, while the low transmittance of carbonyl compounds suggests the presence of hemicellulose.[91]

Furthermore, the presence of C−H bonds, primarily found in alkanes, is associated with reactions resulting in the degradation of hemicellulose. The occurrence of the C═C group, indicating alkenes, facilitates the lignin decomposition reactions. Meanwhile, the C−O group ascribed to carboxylic groups in cellulose and hemicellulose hastens other reactions such as decarboxylation, which breaks glycosidic bonds and forms compounds with lower oxygen content. Generally, the FTIR results in this study revealed that the biomass samples primarily consisted of alkanes. This would enhance the energy-generating potential of bio-oil.

https://doi.org/10.1021/acsomega.3c05656
ACS Omega 2023, 8, 43771−43791

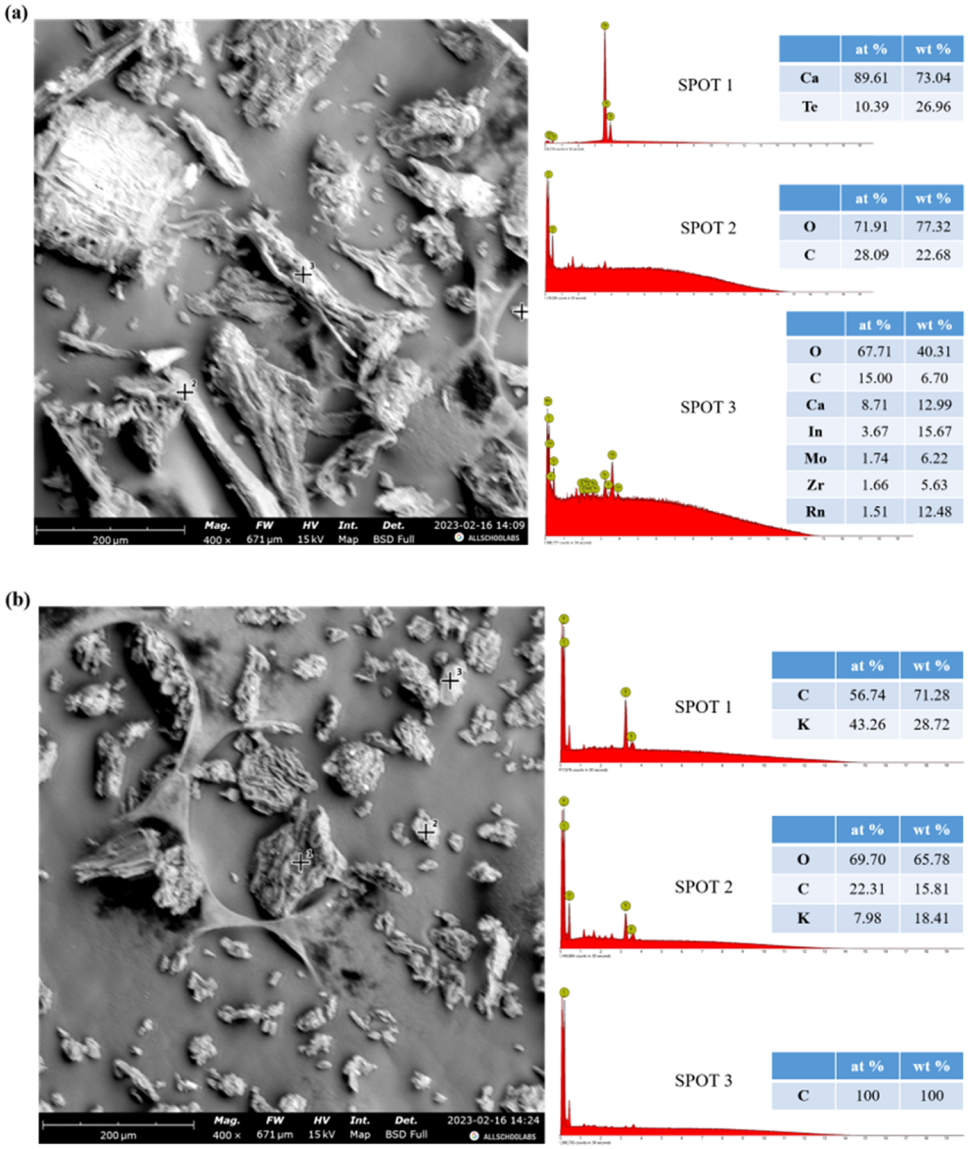

Figure 11. Micrographs and elemental composition of (a) sawdust and (b) *I. coccinea*.

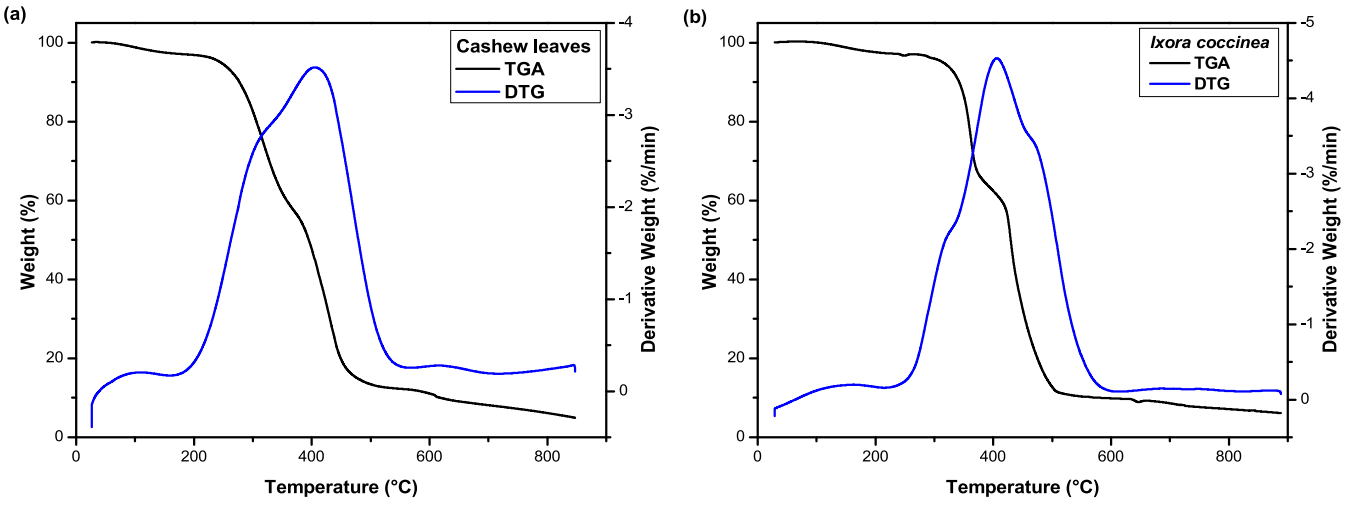

Figure 12. TG and DTG curves of (a) cashew leaves and (b) *I. coccinea*.

https://doi.org/10.1021/acsomega.3c05656
ACS Omega 2023, 8, 43771−43791

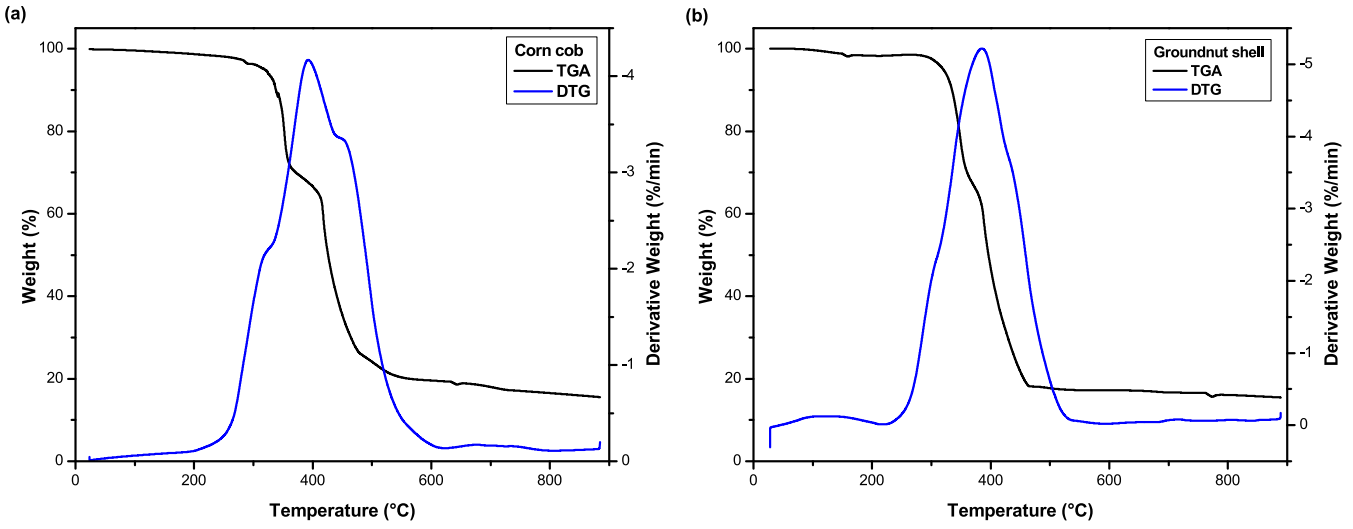

Figure 13. TG and DTG curves of (a) corncob and (b) groundnut shell.

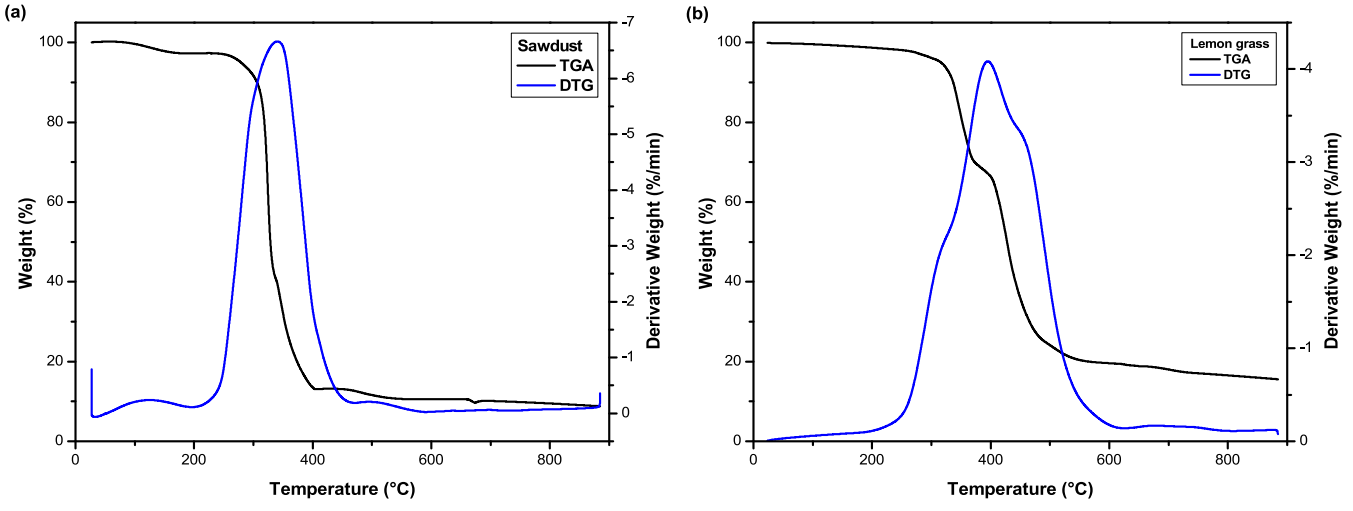

Figure 14. TG and DTG curves of (a) sawdust and (b) lemongrass.

3.3. Scanning Electron Microscopy–Energy-Dispersive X-ray Spectroscopy (SEM-EDS). The micrographs and EDX spectra of the biomass samples are presented in Figures 9 and 11. Expectedly, EDX analysis revealed that carbon and oxygen were the predominant elements in all samples owing to their organic nature. The existence of mineral matter within biomass has been found to exert a beneficial influence during the combustion and pyrolysis processes.[63] In the SEM images, lighter areas indicated a higher concentration of a corresponding element than a dark area.[97]

Cashew leaves exhibited a distinctive honeycomb-like structure with pores, as shown in Figure 9a. Figure 9b shows the fibrous nature of lemongrass, where elongated fibers were observed. Adeleke et al.[98] opined that the fibrous nature of biomass makes its grindability difficult. Other samples also exhibited fibrous characteristics. The SEM image of sawdust (Figure 11a) also revealed a spongy-form structure. This accounts for its hydrophilic nature and tendency for moisture absorption from the environment.[98] This characteristic must be considered when handling and storing sawdust.

As observed from the micrographs in Figures 10 and 11, the samples showed irregular and agglomerated shapes. Although few pores were observed in the SEM image of the corncob (Figure 10a), no clear pores were visible in the micrographs of lemongrass, sawdust, peanut shells, and *I. coccinea*. The absence of pores suggests that these samples were analyzed in their raw form without undergoing any pretreatment procedures.[45]

3.4. Thermogravimetric Analysis (TGA). TGA (pyrolytic decomposition of biomass) provides information about the thermal behavior of biomass. Biomass is a combination of three primary polymeric components, namely, cellulose, hemicellulose, and lignin, along with smaller amounts of nonstructural materials called extractives.[99] Figures 12, 13, and 14 depict the combined TGA and DTG (derivative thermogravimetric) curves at a heating rate of 15 °C/min. These curves are necessary because cellulose, hemicellulose, and lignin exhibit different decomposition behavior.[10,99] According to Mallick et al.,[96] the order of thermal degradation occurrence is hemicellulose > cellulose > lignin. The degradation trend consists mainly of three regions, namely, dehydration, devolatilization, and char formation.[41,63]

The initial region (between 30 and 150 °C) is attributed to weight loss owing to moisture evaporation and light volatile compounds degradation.[98] Between 166 and 277 °C, no significant weight loss was observed. However, above 220 °C (devolatilization stage), the degradation of hemicellulose,

https://doi.org/10.1021/acsomega.3c05656
ACS Omega 2023, 8, 43771−43791

cellulose, and lignin occurs, and this corresponds to the active stage of pyrolysis.[100] Devolatilization is caused by the thermal breakdown of weak bonds within the polymeric structure of the biomass components; hence, more stronger and stable bond formation replace them.[99] Hemicellulose decomposition occurs first, being the least stable of the polymeric biomass. Hemicellulose decomposes at a range of 180−315 °C.[96,101] A pronounced DTG peak was observed between 335 and 410 °C, signifying the degradation of cellulose.[98,102] In an inert atmosphere, this peak is connected to macromolecule formation which contains rings having double bonds.[103] Lignin decomposition typically occurs within 470−900 °C.[10] However, the lignin decomposition has been reported to range from 195 to 500 °C.[98,104] In this study, it was observed that for all of the biomass investigated, the highest degree of volatilization occurred during the active pyrolytic zone (second stage).

The devolatilization parameters (T_{onset}, T_{peak}, DTG_{peak},T_{offset}, and $T_{burnout}$) for the primary decomposition region of the samples are shown in Table 2. T_{onset} signifies the temperature at which devolatilization begins and is an indicator of a material's ease of thermal ignition.[34] In this study, T_{onset} ranged between 201 and 252 °C for the different biomass samples, with cashew leaves being the first to decompose, reflecting its volatility. This agrees with the result of proximate analysis which indicated that cashew leaves exhibited the highest volatile matter. Similar T_{onset} were reported by Yao et al.[105] for various biomass. T_{peak} refers to the temperature of decomposition of biomass polymeric components. The end of devolatilization (cellulose degradation) is indicated by T_{offset},[34] and this parameter is theoretically useful for the design of pyrolysers.[106]

Table 2 also shows that cashew leaves had the highest rate of weight loss (−3.518%/min) at a temperature (T_{peak}) of 407 °C. The variations in the maximum rate of weight loss (DTG_{peak}) and T_{peak} are generally attributed to the reactivity of the biomass, where higher volatility corresponds to increased reactivity.[106] When the weight loss of the samples reaches a relatively stable state, it is referred to as the $T_{burnout}$, and this is indicative of passive pyrolysis.[98]

Table 2. Devolatilization Parameters

	T_{onset} (°C)	T_{peak} (°C)	DTG_{peak} (%/min)	T_{offset} (°C)	$T_{burnout}$ (°C)
cashew leaves	201	407	−3.518	546	634
lemongrass	224	394	−4.083	587	716
corncob	252	392	−4.169	590	718
groundnut shell	230	384	−5.218	532	658
sawdust	218	340	−6.662	503	651
I. coccinea	241	405	−4.530	578	718

3.5. X-ray Fluorescence (XRF). Understanding the composition of inorganic elements in biomass is important for assessing its combustion behavior within furnaces, as it directly impacts corrosion and the deposition of ash on some parts of the facility.[107] Table 3 displays the metal oxide composition of the biomass as analyzed by XRF. The classification of ash composition is typically based on the main constituents present in its mineral composition.[108] From Table 3, it is obvious that the major oxides in the investigated biomass samples are SiO_2, Fe_2O_3, P_2O_5, SO_3, CaO, MgO, K_2O, Al_2O_3, and Cl. The ternary-phase diagram showing the relationship between Ca−K_2O−P_2O_5 and MgO−K_2O−P_2O_5 is presented in Figure 15. The presence of ash-forming

Table 3. Weight Compositions of Oxides of Trace Elements in the Samples

	cashew leaves	lemongrass	corncob	groundnut shell	sawdust	*I. coccinea*
SiO_2	31.513	28.376	40.890	20.080	14.796	5.078
V_2O_5	0.032	0.022	0.000	0.048	0.001	0.000
Cr_2O_3	0.054	0.065	0.239	0.095	0.033	0.009
MnO	2.189	0.622	0.252	0.845	0.065	0.140
Fe_2O_3	3.724	3.483	1.375	8.776	1.074	2.037
Co_3O_4	0.020	0.029	0.042	0.091	0.038	0.034
NiO	0.004	0.031	0.027	0.053	0.011	0.003
CuO	0.440	0.394	0.459	0.901	0.270	0.475
Nb_2O_3	0.078	0.049	0.056	0.141	0.028	0.120
WO_3	0.024	0.015	0.035	0.046	0.017	0.052
P_2O_5	0.556	1.290	1.406	0.124	0.000	1.636
SO_3	4.304	2.495	3.409	2.836	0.000	3.602
CaO	22.707	34.632	6.681	25.028	58.184	17.212
MgO	0.000	0.000	0.653	1.810	0.889	13.644
K_2O	19.832	15.783	23.456	16.355	0.413	39.320
BaO	0.076	0.000	0.079	0.000	0.025	0.095
Al_2O_3	10.704	6.220	12.901	15.571	7.986	7.286
Ta_2O_5	0.045	0.000	0.000	0.000	0.014	0.000
TiO_2	0.588	0.583	0.194	2.420	0.079	0.161
ZnO	0.131	0.154	0.414	0.254	0.069	0.088
Ag_2O	0.000	0.023	0.074	0.154	0.023	0.150
Cl	2.965	5.702	7.199	4.136	15.961	6.443
ZrO_2	0.014	0.033	0.027	0.104	0.011	0.0255
SnO_2	0.000	0.000	0.106	0.000	0.000	2.334
MoO_3	0.000	0.000	0.026	0.128	0.013	0.055

https://doi.org/10.1021/acsomega.3c05656
ACS Omega 2023, 8, 43771−43791

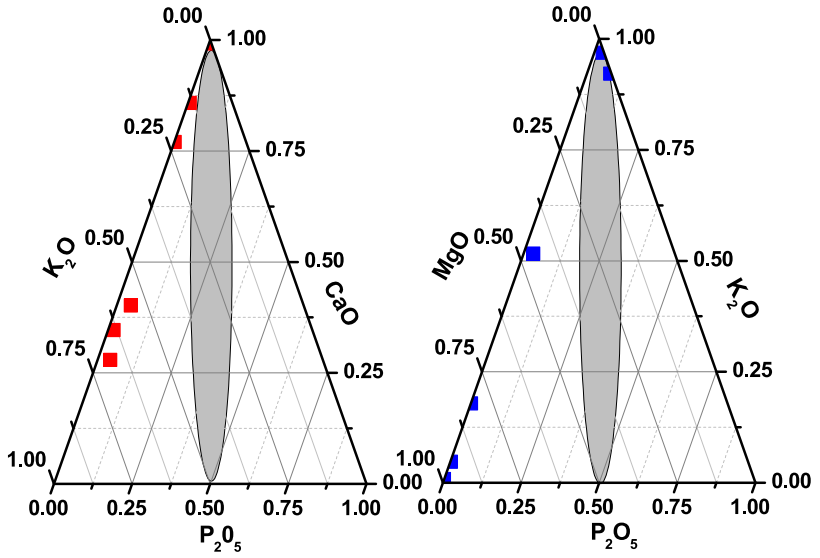

Figure 15. Ternary-phase diagram showing the relationship between $CaO-K_2O-P_2O_5$ and $MgO-K_2O-P_2O_5$.

elements such as Ca, Si, and P has an impact on the release of K into the gas phase. P can combine with K, forming potassium phosphates that remain in the residual ash. Furthermore, the presence of Ca and Mg can also affect K release. One possible explanation for this phenomenon is that Ca primarily binds with Si as calcium silicates, rather than forming potassium calcium silicates. Consequently, Ca may enhance the release of K.[88]

Alkali metals present in biomass aid thermal processes. However, the use of materials with high alkali in a boiler may lead to ash-related issues such as the production of molten salts through vaporization, condensation, and secondary reactions, resulting in a high acid-to-base ratio.[63] For energy purposes, biomass with high K and Ca contents is considered unfavorable. This is because they are readily reactive with other elements, such as silicon (Si), in the formation of alkali compounds having extremely low melting points.[108] Calcium presence acts as a catalyst during the initial stages of pyrolysis, while foaming effects are exhibited by potassium during pyrolysis and enhance the conversion rate.[63]

The slagging indices, calculated using the results (Table 3), are provided in Table 4. These indices serve as indicators of deposition tendencies. Based on criteria, deposition tendency is considered low when Si/Al values and Fe/Ca ratios are below 0.31 or above 3. Conversely, values falling between 0.3 and 3 indicate a high deposition tendency.

Table 4. Slagging Indices of the Samples

	CL	LG	CC	GS	SD	IC
silica-to-alumina ratio	2.94	4.56	3.17	1.29	1.85	0.70
iron calcium ratio	0.16	0.10	0.21	0.35	0.02	0.12
slagging viscosity index	54.39	42.68	82.44	36.05	19.74	13.37

For SiO_2, a low slagging inclination occurs at less than 20%, while a medium slagging inclination occurs within the range of $20 < SiO_2 < 25$ and a high slagging inclination is observed when SiO_2 exceeds 25.[89] For slagging viscosity index (S_r), values in the range of >72, 65−72, and <65 indicate low, medium, and high slagging tendency, respectively.[89] For sulfur (S) content, a low deposition tendency is observed when S is less than 0.6, while a medium deposition tendency occurs within the range of $0.6 < S < 2$, and a high deposition tendency is observed when S exceeds 2.[63]

Comparing the results obtained to the standard in terms of SiO_2 content, Table 3 shows that groundnut shell, sawdust, and *I. coccinea* had values less than 20. This signifies their low likelihood of a low slagging inclination. Considering sulfur content, Table 3 shows that all samples, except for sawdust, had values greater than 2. This signifies a high tendency for deposition during the combustion processes. In Table 4, lemongrass and corncob had silica-to-alumina and iron-to-calcium ratios fall outside the range of 0.3−3, indicating a low likelihood of deposition. The calculated slagging viscosity index (Sr) in Table 4 further reveals corncob as the feedstock having the lowest tendency to slag.

3.6. Fuel Ratio, Ignitability Index, and Combustibility Index. Figure 16c illustrates the fuel ratio (FR) of the investigated samples ranging from 0.06836 (cashew leaves) to 0.32771 (groundnut shell). Notably, this study reports different FRs for corncob (0.28012) and sawdust (0.1641) in comparison to the values obtained by Jia et al.[109] (0.1999 and 0.2835, respectively). Biomass typically exhibits a low FR due to its high VM and relatively low FC content.[110] Fuels having a fuel ratio greater than 2 (FR > 2) may encounter ignition and flammability issues. All the analyzed samples had fuel ratios below 2, indicating their suitability as feedstocks. A low FR in biomass promotes more flaming combustion, rapid burning, and less unburned char.[9,110]

In bio-oil production, feedstocks with lower FRs are preferred due to their higher concentration of VM relative to FC. This composition facilitates easy vaporization and contributes to bio-oil production during pyrolysis, while the FC remains as solid char. During pyrolysis, the thermal decomposition of VM, which primarily contains cellulose and hemicellulose rich in carbon and hydrogen, adds to the formation of bio-oil.[111] Hence, cashew leaves, lemongrass, and sawdust have been identified as more suitable feedstocks for bio-oil production.

The ignitability index (I_I) serves as an indicator of biomass performance under furnace or boiler conditions. Biomass with

https://doi.org/10.1021/acsomega.3c05656
ACS Omega 2023, 8, 43771−43791

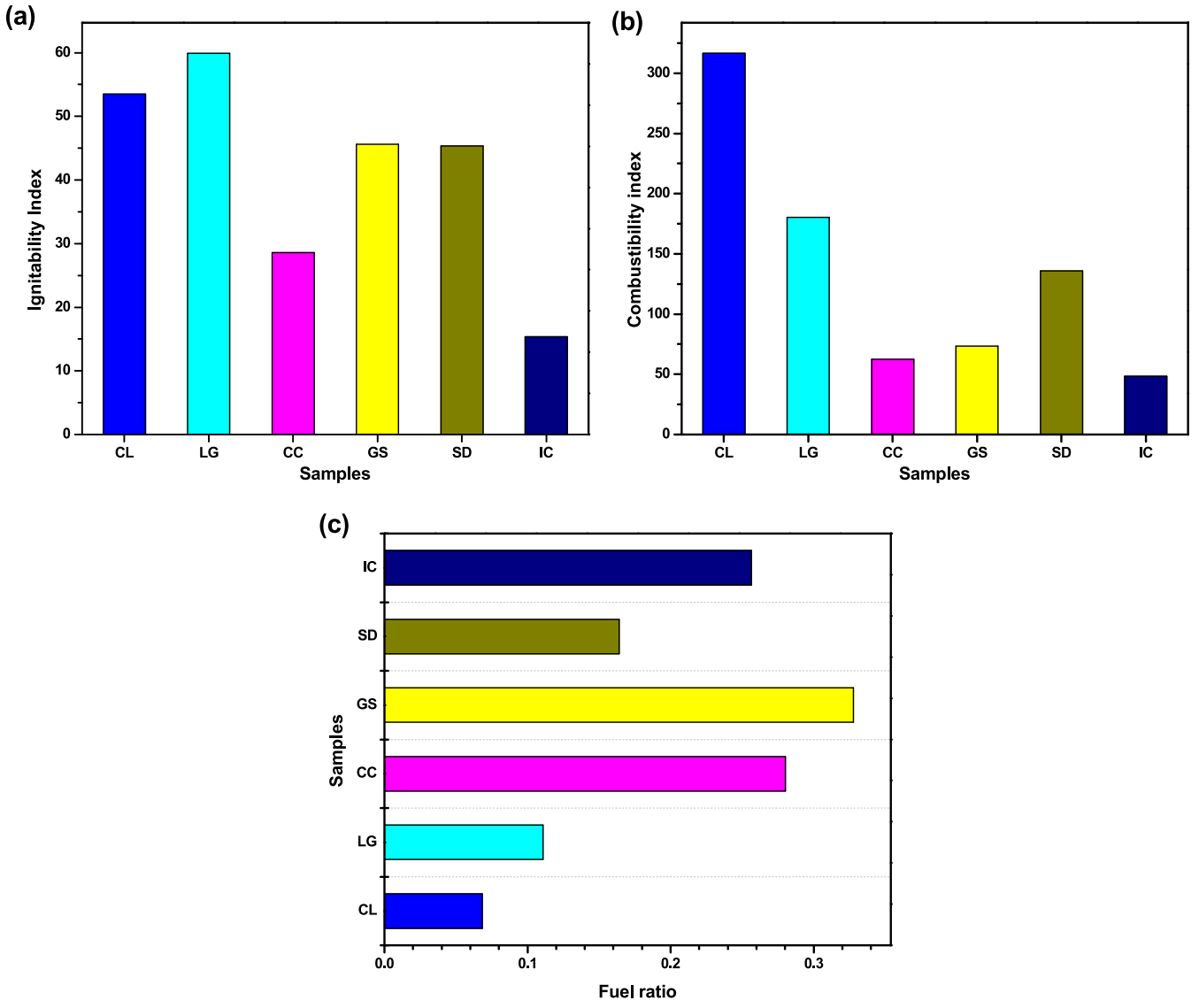

Figure 16. (a) Ignitability index, (b) combustibility index, and (c) fuel ratio of the biomass.

a high I_I facilitates rapid decomposition within pyrolysis plants, enhancing the overall efficiency.[10] In the present study, the ignitability values ranged from 15.38 (*I. coccinea*) to 59.92 (lemongrass) (Figure 16a). Adeleke et al.[98] found that a high FR is often connected with a high ignitability index. According to the findings, if the ignitability index of solid fuel falls below 35, it may pose difficulties in achieving efficient utilization in a boiler. The combustibility indexes of the samples in this study were in the range of 48.24−316.62 MJ/kg (Figure 16b). However, Singh et al.[111] reported that the combustibility index should be lower than 23 MJ/kg.

3.7. H/C (Hydrogen to Carbon) and O/C (Oxygen to Carbon) Atomic Ratios. The quality of a fuel is primarily determined by the H/C and O/C atomic ratios, making them useful parameters for fuel comparison.[112] Saxby[113] noted that the H/C ratio of coal or kerogen serves as an indicator of oil-forming potential during pyrolysis or diagenesis. In this study, the H/C atomic ratios of the samples ranged from 0.67 to 0.87, while the O/C ratios ranged from 0.63 to 1.01. These discoveries align with the established fact that raw biomass generally exhibits higher O/C and H/C ratios.[60] Figure 17 presents a Van Krevelen plot to visualize the location of the biomass samples using the correlation between these ratios. All samples fell within the upper right region of the plot, indicating a higher proportion of oxygenated molecules.[85,114] This confirms the oxygen-rich nature of the biomass materials characterized by higher O/C ratios. Conversely, hydrocarbon-based materials appear toward the lower left region of the plot. Fuels with lower H/C and O/C ratios are generally considered more favorable, as they minimize the loss of energy during combustion, water vapor, and smog formation.[115] Decreasing H/C and O/C atomic ratios correspond to higher energy density and HHV of fuel feedstocks.[9,46,83] This can be attributed to the greater chemical energy stored in C−C bonds compared with C−O bonds.[83] Typically, moving from the upper right to the lower left on the Van Krevelen diagram shows the direction of increasing energy content. Decreasing H/C and O/C atomic ratios also denote an aromaticity increase and a reduction in oxygen-based functional groups such as hydroxyl, ether, carboxyl, and ketone groups in the biomass.[9]

For sawdust, the O/C (1.01) aligns with the O/C ratio (0.96) while the H/C ratio (0.67) contradicts the 0.127 reported by Oluwatosin et al.[89] For corncob, the O/C value

https://doi.org/10.1021/acsomega.3c05656
ACS Omega 2023, 8, 43771−43791

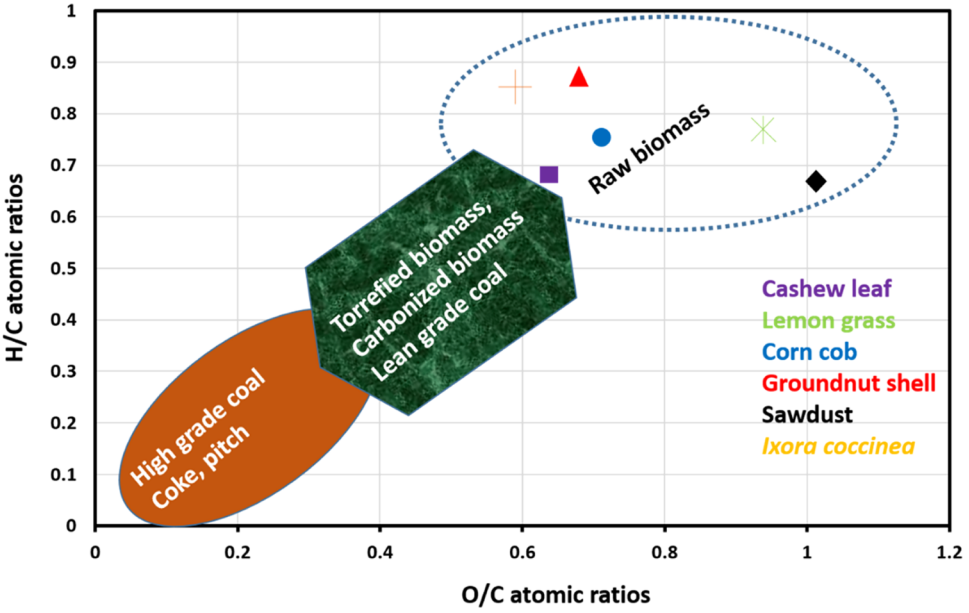

Figure 17. Van Krevelen plot of H/C and O/C atomic ratios.

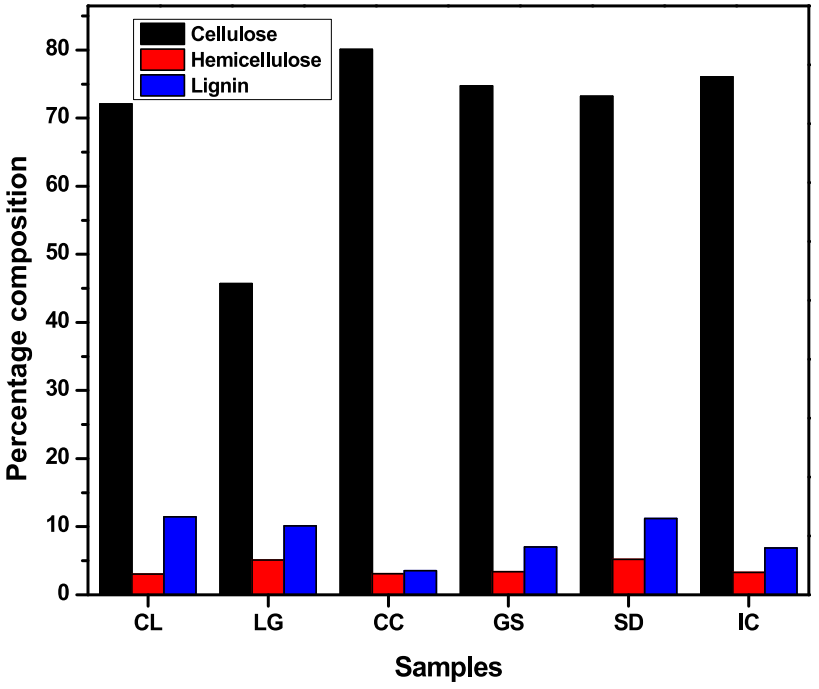

Figure 18. Compositional analyses of the samples.

(0.71) matches that reported for corn stover[85];[85] however, the H/C values (0.76) differ significantly to 1.69. Liu et al.[42] reported the H/C (1.43) and O/C (0.64) atomic ratios for corncob. Gushit et al.[68] reported O/C ratios of 0.69 and 0.62 for *Hibiscus canabinus* and *Vernonia colorata*, respectively, which align with the O/C ratios of 0.68, 0.71, and 0.63 found in this study for groundnut shell, corncob, and cashew leaves, respectively. Hence, it could be inferred that the groundnut shell would have a better burning efficiency owing to its higher H/C atomic ratio (0.87) with respect to other biomass in this study. Also, its higher H/C atomic ratio infers lower carbon dioxide emissions from its combustion.[116] However, with the higher oxygen contents observed in the samples, pretreatment may be required to optimize their conversion into bio-oil.

3.8. Structural Compositional Analyses. The biomass structural compositions are cellulose, hemicellulose, and lignin.[117] Cellulose and hemicellulose collectively make up 60−90% of biomass weight, with cellulose being a linear polymer of glucose and hemicellulose, a complex amorphous polymer. Conversely, lignin is a highly branched and substituted polyaromatic compound, accounting for 10−25% of the weight of the biomass. The average structural composition analysis (Figure 18), demonstrates the range of values for cellulose content (45.71−80.08%), hemicellulose (3.03−5.23%), and lignin (6.89−11.43%).

https://doi.org/10.1021/acsomega.3c05656
ACS Omega 2023, 8, 43771−43791

It was observed from Figure 18 that the biomass samples exhibited higher cellulose over lignin contents, while the hemicellulose content was comparatively lower. This composition indicates the potential suitability of the biomass for pyrolysis, as increased cellulose and hemicellulose contents contribute to a higher pyrolysis rate.[10] Consequently, volatile products, such as bio-oil and noncondensable gases (NCG), are predominantly produced. Conversely, higher lignin content in biomass reduces the pyrolysis rate, leading to an increased yield of biochar.[1]

In addition to these three major polymeric structures, biomass contains some minor constituents. These include ether extract, crude protein, and crude fat, and their proportions in the biomass samples in this study are presented in Table 5.

Table 5. Minor Components of the Biomass Samples

	CL	LG	CC	GS	SD	IC
ether extract	12.34	11.34	19.76	12.02	13.62	10.96
crude protein	3.01	2.98	2.31	3.63	2.27	2.06
crude fat	2.40	1.07	1.63	2.95	1.98	1.18
ash	1.88	1.34	3.52	5.73	1.56	1.36

4. CONCLUSIONS

The following conclusions were derived from the comprehensive set of characterizations carried out in this study. The characterization showed that the investigated biomass had moisture content (MC), volatile matter (VM), ash content (AC), fixed carbon (FC), and higher heating value (HHV) in the range of 5.79−8.28, 68.17−83.24, 1.21−17.2, 5.69−22.34%, and 11.4346−22.1848 MJ/kg, respectively. The carbon contents of the samples investigated are between 40.37 and 47.90%, hydrogen between 4.52 and 6.83%, and oxygen contents between 38.69 and 54.20%. The nitrogen and sulfur contents were in the range of 0.12−3.28 and 0.04−0.19%, respectively, making them environmentally friendly. The thermal decomposition study showed that the highest degree of volatilization occurred during the second stage (devolatilization stage), which corresponds to the active pyrolytic zone, with cashew leaves exhibiting the maximum weight loss rate. The major trace elements found in the biomass, in the form of oxides, included SiO_2, Fe_2O_3, P_2O_5, SO_3, CaO, MgO, K_2O, Al_2O_3, and Cl. The high concentration of K and Ca is considered unfavorable due to their tendency to react with other elements. Calcium's presence serves as a catalyst during the initial stages of pyrolysis, while potassium leads to foaming effects during pyrolysis and enhances the conversion rate. The compositional analyses revealed that the biomass samples were composed of cellulose compared with hemicellulose and lignin. The presence of high cellulose content favors the production of bio-oil. The samples had good flammability and ignition characteristics. It is suggested that other biomass studies of Nigerian origin should be characterized and stored in a database. Further studies on the various combinations of biomass materials for sustainable energy use should be considered. Moreover, feasibility studies that involve the techno-economical and environmental impacts of biomass in some developed energy systems should be investigated.

AUTHOR INFORMATION

Corresponding Author

Prabhu Paramasivam − *Department of Mechanical Engineering, College of Engineering and Technology, Mattu University, Mettu 318, Ethiopia;* orcid.org/0000-0002-2397-0873; Email: prabhu.paramasivam@meu.edu.et

Authors

Asmau M. Yahya − *Department of Petroleum and Gas Engineering, Nile University of Nigeria, Abuja 900001, Nigeria*

Adekunle A. Adeleke − *Department of Mechanical Engineering, Nile University of Nigeria, Abuja 900001, Nigeria*

Petrus Nzerem − *Department of Petroleum and Gas Engineering, Nile University of Nigeria, Abuja 900001, Nigeria*

Peter P. Ikubanni − *Department of Mechanical Engineering, Landmark University, Omu Aran 251103, Nigeria*

Salihu Ayuba − *Department of Petroleum and Gas Engineering, Nile University of Nigeria, Abuja 900001, Nigeria*

Hauwa A. Rasheed − *Department of Industrial Chemistry, Nile University of Nigeria, Abuja 900001, Nigeria*

Abdullahi Gimba − *Department of Petroleum and Gas Engineering, Nile University of Nigeria, Abuja 900001, Nigeria*

Ikechukwu Okafor − *Department of Petroleum and Gas Engineering, Nile University of Nigeria, Abuja 900001, Nigeria*

Jude A. Okolie − *Gallogly College of Engineering, University of Oklahoma, Norman, Oklahoma 73019, United States*

Complete contact information is available at: https://pubs.acs.org/10.1021/acsomega.3c05656

Notes

The authors declare no competing financial interest.

ACKNOWLEDGMENTS

The authors appreciate the management of Nile University of Nigeria, Abuja, for providing some of the equipment used in carrying out this study. The authors also thank Mattu University, Ethiopia, for their support.

REFERENCES

(1) Guedes, R. E.; Luna, A. S.; Torres, A. R. Operating parameters for bio-oil production in biomass pyrolysis: A review. *J. Anal. Appl. Pyrolysis* **2018**, *129*, 134−149.

(2) World Population Projected to Reach 9.8 Billion in 2050, and 11.2 Billion in 2100, United Nation, 2017 https://www.un.org/en/desa/world-population-projected-reach-98-billion-2050-and-112-billion-2100#:~:text=COVID%2D19-,World%20population%20projected%20to%20reach%209.8%20billion%20in%202050%2C%20and,Nations%20report%20being%20launched%20todayhttps://www.un.org/en/desa/world-population-projected-reach-98-billion-2050-and-112-billion-2100#:~:text=COVID%2D19-,World%20population%20projected%20to%20reach%209.8%20billion%20in%202050%2C%20and,Nations%20report%20being%20launched%20today. (Accessed February 25, 2023).

(3) Atuguba, R. A.; Tuokuu, F. X. D. Ghana's renewable energy agenda: Legislative drafting in search of policy paralysis. *Energy Res. Soc. Sci.* **2020**, *64*, No. 101453.

https://doi.org/10.1021/acsomega.3c05656
ACS Omega 2023, 8, 43771−43791

(4) Onokwai, A. O.; Okonkwo, U. C.; Osueke, C. O.; Olayanju, T.; Ezugwu, C. A.; Diarah, R. S.; Banjo, S. O.; Onokpite, E.; Olabamiji, T. S.; Ibiwoye, M.; James, J. A.; Nnodim, T. C. Thermal analysis of solar box cooker in Omu-Aran metropolis. *J. Phys: Conf. Ser.* **2019**, *1378*, No. 032065.
(5) Nnodim, C. T.; Kpu, G. C.; Okhuegbe, S. N.; Ajani, A. A.; Adebayo, S.; Diarah, R. S.; Aliyu, S. J.; Onokwai, A. O.; Osueke, C. O. Figures of merit for wind and solar PV integration in electricity grids. *J. Sci. Ind. Res.* **2022**, *81*, 349−357.
(6) Chukwuneke, J. L.; Ewulonu, M. C.; Chukwujike, I. C.; Okolie, P. C. Physico-chemical analysis of pyrolyzed bio-oil from *Swietenia macrophylla* (mahogany) wood. *Heliyon* **2019**, *5*, No. e01790.
(7) Okafor, C. C.; Nzekwe, C. A.; Ajaero, C.; Ibekwe, J. C.; Otunomo, F. A. Biomass utilization for energy production in Nigeria: A review. *Cleaner Energy Syst.* **2022**, *3*, No. 100043.
(8) Sokan-Adeaga, A. A.; Ana, G. R. E. E. A comprehensive review of biomass resources and biofuel production in Nigeria: potential and prospects. *Rev. Environ. Health* **2015**, *30*, 143−162.
(9) Adeleke, A. A.; Odusote, J. K.; Ikubanni, P. P.; Lasode, O. A.; Malathi, M.; Paswan, D. The ignitability, fuel ratio and ash fusion temperatures of torrefied woody biomass. *Heliyon* **2020**, *6*, No. e03582.
(10) Onokwai, A. O.; Ajisegiri, E. S. A.; Okokpujie, I. P.; Ibikunle, R.; Oki, M.; Dirisu, J. O. Characterization of lignocellulose biomass based on proximate, ultimate, structural composition, and thermal analysis. *Mater. Today: Proc.* **2022**, *65*, 2156−2162.
(11) International Energy Agency Global CO_2 Emissions Rebounded to Their Highest Level in History in 2021, 2022. https://www.iea.org/news/global-co2-emissions-rebounded-to-their-highest-level-in-history-in-2021. (Accessed February 25, 2023).
(12) Jekayinfa, S. O.; Orisaleye, J.; Pecenka, R. An Assessment of potential resources for biomass energy in Nigeria. *Resources* **2020**, *9*, No. 92.
(13) Awoyale, A. A.; Lokhat, D. Experimental determination of the effects of pretreatment on selected Nigerian lignocellulosic biomass in bioethanol production. *Sci. Rep.* **2021**, *11*, No. 557.
(14) Jamil, F.; Aslam, M.; Al-Muhtaseb, A. H.; Bokhari, A.; Rafiq, S.; Khan, Z.; Inayat, A.; Ahmed, A.; Hossain, S.; Khurram, M.; Bakar, M. S. A. Greener and sustainable production of bioethylene from bioethanol: current status, opportunities and perspectives. *Rev. Chem. Eng.* **2022**, *38*, 185−207.
(15) Ahmed, A.; Bakar, M. S. A.; Azad, A. K.; Sukri, R. S.; Mahlia, T. M. I. Potential thermochemical conversion of bioenergy from *Acacia species* in Brunei Darussalam: A review. *Renewable Sustainable Energy Rev.* **2018**, *82*, 3060−3076.
(16) Ahmed, A.; Bakar, M. S. A.; Sukri, R. S.; Hussain, M.; Farooq, A.; Moogi, S.; Park, Y. Sawdust pyrolysis from the furniture industry in an auger pyrolysis reactor system for biochar and bio-oil production. *Energy Convers. Manage.* **2020**, *226*, No. 113502.
(17) Obi, F.; Ugwuishiwu, B.; Nwakaire, J. Agricultural waste concept, generation, utilization and management. *Niger. J. Technol.* **2016**, *35*, 957−964.
(18) Ibeto, C. N.; Anisha, M.; Anyanwu, C. N. Evaluation of the fuel properties and pollution potentials of lignite coal and pellets of its blends with different biowastes. *Am. Chem. Sci. J.* **2016**, *14*, 1−12.
(19) IEA. Transport Biofuels − Analysis, 2023. https://www.iea.org/reports/transport-biofuels/.
(20) Pang, S. Advances in thermochemical conversion of woody biomass to energy, fuels and chemicals. *Biotechnol. Adv.* **2019**, *37*, 589−597.
(21) Lee, K. T.; Ofori-Boateng, C. *Sustainability of Biofuel Production from Oil Palm Biomass*; Springer: Singapore, 2013.
(22) Gao, N.; Kamran, K.; Quan, C.; Williams, P. Thermochemical conversion of sewage sludge: A critical review. *Prog. Energy Combust. Sci.* **2020**, *79*, No. 100843.
(23) Wang, S.; Zhao, S. G.; Uzoejinwa, B. B.; Zheng, A.; Wang, Q.; Huang, J.; Abomohra, A. E. A state-of-the-art review on dual purpose seaweeds utilization for wastewater treatment and crude bio-oil production. *Energy Convers. Manage.* **2020**, *222*, No. 113253.
(24) Ibrahim, M. D.; Abakr, Y. A.; Gan, S.; Thangalazhy-Gopakumar, S. Physicochemical analysis and intermediate pyrolysis of bambara groundnut shell (BGS), sweet sorghum stalk (SSS), and shea nutshell (SNS). *Environ. Technol.* **2022**, 1−14.
(25) Lyu, G.; Wu, S.; Zhang, H. Estimation and comparison of bio-oil components from different pyrolysis conditions. *Front. Energy Res.* **2015**, *3*, No. 28, DOI: 10.3389/fenrg.2015.00028.
(26) Hu, X.; Gholizadeh, M. Progress of the applications of bio-oil. *Renewable Sustainable Energy Rev.* **2020**, *134*, No. 110124.
(27) Ezealigo, U. S.; Otoijamun, I.; Onwualu, A. P. Electricity and biofuel production from biomass in Nigeria: Prospects, challenges and way forward. *IOP Conf. Ser.: Earth Environ. Sci.* **2021**, *730*, No. 012035.
(28) ASTM E871−82. *Standard Test Method for Moisture Analysis of Particulate Wood Fuels*, ASTM International2013.
(29) ASTM E872−82. *Standard Test Method for Volatile Matter in the Analysis of Particulate Wood Fuels*; ASTM International, 2019.
(30) ASTM E1755−01. *Standard Test Method for Ash in Biomass, ASTM Fuels*, ASTM International2015.
(31) ASTM D5373−16. *Standard Test Methods for Determination of Carbon, Hydrogen and Nitrogen in Analysis Samples of Coal and Carbon in Analysis Samples of Coal and Coke*, ASTM International2016.
(32) ASTM D4239−11. *Standard Test Method for Sulphur in Sample of Coal and Coke Using High Temperature Tube Furnace Combustion*, ASTM International2011.
(33) ASTM D5373−16. *Standard Test Methods for Gross Calorific Value of Coal and Coke*, ASTM International2016.
(34) Nyakuma, B. B.; Ngadi, N.; Oladokun, O.; Bello, A.; Hambali, H.; Abdullah, T. A. T.; Wong, K. L. Review of the fuel properties, characterisation techniques, and pre-treatment technologies for oil palm empty fruit bunches. *Biomass Convers. Biorefin.* **2023**, *13*, 471−497.
(35) Mitchual, S. J.; Frimpong-Mensah, K.; Darkwa, N. A. Evaluation of fuel properties of six tropical hardwood timber species for briquettes. *J. Sustainable Bioenergy Syst.* **2014**, *04*, No. 44225.
(36) Bhavsar, P.; Jagadale, M.; Khandetod, Y. P.; Mohod, A. G. Proximate analysis of selected non-woody biomass. *Int. J. Current Microbiol. Appl. Sci.* **2018**, *7*, 2846−2849.
(37) Nithiya, K.; Subramanian, P.; Ramesh, D.; Uma, D.; Surendrakumar, A. Bio-oil production from groundnut shell fast pyrolysis in spouted bed reactor. *Pollut. Res.* **2022**, *41*, 362−366.
(38) Rapheal, I. A.; Moki, E. C.; Muhammad, A.; Mohammed, G.; Hassan, L. G.; BirninYauri, A. U. Physico-chemical and combustion analyses of bio-briquettes from biochar produced from pyrolysis of groundnut shell. *Int. J. Adv. Chem.* **2021**, *9*, 74−79.
(39) Varma, A. K.; Singh, S.; Rathore, A. K.; Thakur, L. S.; Shankar, R.; Mondal, P. Investigation of kinetic and thermodynamic parameters for pyrolysis of peanut shell using thermogravimetric analysis. *Biomass Convers. Biorefin.* **2022**, *12*, 4877−4888.
(40) Pawar, A. Y.; Panwar, N. L. Experimental investigation on biochar from groundnut shell in a continuous production system. *Biomass Convers. Biorefin.* **2022**, *12*, 1093−1103.
(41) Collins, S. M.; Ghodke, P. Kinetic parameter evaluation of groundnut shell pyrolysis through use of thermogravimetric analysis. *J. Environ. Chem. Eng.* **2018**, *6*, 4736−4742.
(42) Liu, X.; Zhang, Y.; Li, Z.; Feng, R.; Zhang, Y. Characterization of corncob-derived biochar and pyrolysis kinetics in comparison with corn stalk and sawdust. *Bioresour. Technol.* **2014**, *170*, 76−82.
(43) Varma, A. K.; Thakur, L. S.; Shankar, R.; Mondal, P. Pyrolysis of wood sawdust: Effects of process parameters on products yield and characterization of products. *Waste Manage.* **2019**, *89*, 224−235.
(44) Madhu, P.; Livingston, T. S.; Manickam, I. N. Fixed bed pyrolysis of lemongrass (*Cymbopogon flexuosus*): Bio-oil production and characterization. *Energy Sources, Part A* **2017**, *39*, 1359−1368.
(45) Anukam, A. I.; Goso, B. P.; Okoh, O. O.; Mamphweli, S. Studies on characterization of corn cob for application in a gasification process for energy production. *J. Chem.* **2017**, *2017*, No. 6478389.

https://doi.org/10.1021/acsomega.3c05656
ACS Omega 2023, 8, 43771−43791

(46) Holtmeyer, M. L.; Li, G.; Kumfer, B. M.; Li, S.; Axelbaum, R. L. The impact of biomass cofiring on volatile flame length. *Energy Fuels* **2013**, *27*, 7762−7771.
(47) Basu, P. Economic Issues of Biomass Energy Conversion. In *Biomass Gasification, Pyrolysis and Torrefaction*, 2nd ed.; Academic Press: London, 2013.
(48) Liu, X.; Chen, M.; Wei, Y. Kinetics based on two-stage scheme for co-combustion of herbaceous biomass and bituminous coal. *Fuel* **2015**, *143*, 577−585.
(49) Sharma, P.; Sivaramakrishnaiah, M.; Deepanraj, B.; Saravanan, R.; Reddy, M. V. A novel optimization approach for biohydrogen production using algal biomass. *Int. J. Hydrogen Energy* **2022**, DOI: 10.1016/j.ijhydene.2022.09.274.
(50) Speight, J. G. *The Chemistry and Technology of Coal*, 3rd ed.; CRC Press: Boca Raton, 2012.
(51) Akogun, O. A.; Waheed, M. A. Property upgrades of some raw Nigerian biomass through torrefaction pre-treatment - A review. *J. Phys.: Conf. Ser.* **2019**, *1378*, No. 032026.
(52) Mensah, I.; Ahiekpor, J. C.; Herold, N.; Bensah, E. C.; Pfriem, A.; Antwi, E.; Amponsem, B. Biomass and plastic co-pyrolysis for syngas production: Characterisation of *Celtis mildbraedii* sawdust as a potential feedstock. *Sci. Afr.* **2022**, *16*, No. e01208.
(53) Mamaeva, A.; Tahmasebi, A.; Yu, J. The effects of mineral salt catalysts on selectivity of phenolic compounds in bio-oil during microwave pyrolysis of peanut shell. *Korean J. Chem. Eng.* **2017**, *34*, 672−680.
(54) Kuhe, A.; Aliyu, S. J. Gasification of 'Loose' groundnut shells in a throathless downdraft gasifier. *Int. J. Renewable Energy Dev.* **2015**, *4*, 125−130.
(55) Radhakrishnan, N.; Venkadesan, G. Pyrolysis of groundnut shell biomass to produce bio-oil. *J. Chem. Pharm. Sci.* **2015**, *9*, 34−36.
(56) Abatyough, M. T.; Ajibola, V. O.; Agbaji, E. B.; Yashim, Z. I. Properties of upgraded bio-oil from pyrolysis of waste corn cobs. *J. Sustainability Environ. Manage.* **2022**, *1*, 120−128.
(57) Shariff, A.; Aziz, N. F. A.; Ismail, N.; Abdullah, N. Corn cob as a potential feedstock for slow pyrolysis of biomass. *J. Phys. Sci.* **2016**, *27*, 123−137.
(58) Ajobo, J. A. Densification characteristics of groundnut shell. *Int. J. Mech. Indus. Technol.* **2014**, *2*, 150−154.
(59) Vassilev, S. V.; Baxter, D. V.; Andersen, L. B.; Vassileva, C. G. An overview of the composition and application of biomass ash. Part 1. Phase−mineral and chemical composition and classification. *Fuel* **2013**, *105*, 40−76.
(60) Adeleke, A. A.; Odusote, J. K.; Ikubanni, P. P.; Lasode, O. A.; Malathi, M.; Paswan, D. Essential basics on biomass torrefaction, densification and utilization. *Int. J. Energy Res.* **2021**, *45*, 1375−1395.
(61) Dai, L.; Zhou, N.; Li, H.; Deng, W.; Cheng, Y.; Wang, Y.; Liu, Y.; Cobb, K.; Lei, H.; Chen, P.; Ruan, R. Recent advances in improving lignocellulosic biomass-based bio-oil production. *J. Anal. Appl. Pyrolysis* **2020**, *149*, No. 104845.
(62) Chang, S. H. An overview of empty fruit bunch from oil palm as feedstock for bio-oil production. *Biomass Bioenergy* **2014**, *62*, 174−181.
(63) Mishra, R. K.; Mohanty, K. Characterization of non-edible lignocellulosic biomass in terms of their candidacy towards alternative renewable fuels. *Biomass Convers. Biorefin.* **2018**, *8*, 799−812.
(64) He, X.; Liu, Z.; Niu, W.; Yang, L.; Zhou, T.; Qin, D.; Niu, Z.; Yuan, Q. Effects of pyrolysis temperature on the physicochemical properties of gas and biochar obtained from pyrolysis of crop residues. *Energy* **2018**, *143*, 746−756.
(65) Demirbas, A. Effects of moisture and hydrogen content on the heating value of fuels. *Energy Sources, Part A* **2007**, *29*, 649−655.
(66) Javier, S.; Jesus, F. *Role of Bioenergy in the Bioeconomy: Resources, Technologies, Sustainability and Policy*; Academic Press: London, 2019.
(67) ONORM M7135 Compressed Wood or Compressed Bark in Natural State, Pellets and Briquettes *Requir. Test Specif.* 2003.
(68) Gushit, J. S.; Shimuan, J. T.; Ajana, M. O. Studies on the energy properties and fuel potentials of selected indigenously processed bio-resources used as sources of sustainable fuel in North Central Nigeria. *J. Res. For., Wildl. Environ.* **2019**, *9*, 12−17.
(69) Omar, R.; Idris, A. M.; Yunus, R.; Khalid, K.; Isma, M. I. A. Characterization of empty fruit bunch for microwave-assisted pyrolysis. *Fuel* **2011**, *90*, 1536−1544.
(70) Lee, Y.; Park, J.; Ryu, C.; Gang, K. S.; Yang, W. J.; Park, Y.; Jung, J.; Hyun, S. Comparison of biochar properties from biomass residues produced by slow pyrolysis at 500°C. *Bioresour. Technol.* **2013**, *148*, 196−201.
(71) Said, Z.; Sharma, P.; Bora, B. J.; Nguyen, V. N.; Bui, T. A. E.; Nguyen, D. T.; Dinh, X. T.; Nguyen, X. P. Modeling-optimization of performance and emission characteristics of dual-fuel engine powered with pilot diesel and agricultural-food waste-derived biogas. *Int. J. Hydrogen Energy* **2023**, *48*, 6761−6777.
(72) Abnisa, F.; Arami-Niya, A.; Daud, W. M. A. W.; Sahu, J. K. Characterization of bio-oil and bio-char from pyrolysis of palm oil wastes. *BioEnergy Res.* **2013**, *6*, 830−840.
(73) Razuan, R.; Chen, Q. Y.; Zhang, X. Y.; Sharifi, V. N.; Swithenbank, J. Pyrolysis and combustion of oil palm stone and palm kernel cake in fixed-bed reactors. *Bioresour. Technol.* **2010**, *101*, 4622−4629.
(74) da Silva, D. A.; Hansted, A. L. S.; Nakashima, G. T.; Padilla, E. R. D.; Pereira, J. C. R.; Yamaji, F. M. Volatile matter values change according to the standard utilized? *Res, Soc. Dev.* **2021**, *10*, No. e291101220476.
(75) Ogunjobi, J. K.; Lajide, L. Characterisation of bio-oil and bio-char from slow-pyrolysed Nigerian yellow and white corn cobs. *J. Sustainable Energy Environ.* **2013**, *4*, 77−84.
(76) Medic, D.; Darr, M. J.; Shah, A. M.; Rahn, S. J. The effects of particle size, different corn stover components, and gas residence time on torrefaction of corn stover. *Energies* **2012**, *5*, 1199−1214.
(77) Demiral, İ.; Eryazıcı, A.; Şensöz, S. Bio-oil production from pyrolysis of corncob (*Zea mays* L.). *Biomass Bioenergy* **2012**, *36*, 43−49.
(78) Elehinafe, F. B.; Okedere, O. B.; Odunlami, O. A.; Mamudu, A. O.; Fakinle, B. S. Proximate analysis of the properties of some southwestern Nigeria sawdust of different wood species. *Int. J. Civil Eng. Technol.* **2019**, *10*, 51−59.
(79) Rathod, N.; Jain, S.; Patel, M. R. Thermodynamic analysis of biochar produced from groundnut shell through slow pyrolysis. *Energy Nexus* **2023**, *9*, No. 100177.
(80) Inna, S.; Amadou, O. A.; Yvette, J. N.; Cârâc, G.; Mihaela, R. D.; Richard, K. Assessment of efficient thermal conversion technologies and HHV from compositional characteristics of cassava peelings, plantain peelings and corn cobs. *Energy Res. J.* **2022**, *13*, 30−41.
(81) Özyuğuran, A.; Yaman, S. Prediction of calorific value of biomass from proximate analysis. *Energy Procedia* **2017**, *107*, 130−136.
(82) Shaba, M. I. Production of bioenergy from rice-melon husk co-digested with cow dung as innoculant. *Agric. Eng. Int.: CIGR J.* **2020**, *22*, 108−117.
(83) Singh, Y. D.; Mahanta, P.; Bora, U. Comprehensive characterization of lignocellulosic biomass through proximate, ultimate and compositional analysis for bioenergy production. *Renewable Energy* **2017**, *103*, 490−500.
(84) Trninić, M.; Wang, L.; Várhegyi, G.; Grønli, M.; Skreiberg, Ø. Kinetics of corncob pyrolysis. *Energy Fuels* **2012**, *26*, 2005−2013.
(85) Capunitan, J. A.; Capareda, S. C. Assessing the potential for biofuel production of corn stover pyrolysis using a pressurized batch reactor. *Fuel* **2012**, *95*, 563−572.
(86) Sharma, P.; Sivaramakrishnaiah, M.; Deepanraj, B.; Saravanan, R.; Reddy, M. V. A novel optimization approach for biohydrogen production using algal biomass *Int. J. Hydrogen Energy* 2022, DOI: 10.1016/j.ijhydene.2022.09.274.
(87) Park, C.; Roy, P. S.; Kim, S. W. Current Developments in Thermochemical Conversion of Biomass to Fuels and Chemicals. In *Gasification for Low-Grade Feedstock*; Yun, Y., Ed.; InTechOpen Ltd.: London, 2018.

https://doi.org/10.1021/acsomega.3c05656
ACS Omega 2023, 8, 43771−43791

(88) Sommersacher, P.; Brunner, T.; Obernberger, I. Fuel indexes: A novel method for the evaluation of relevant combustion properties of new biomass fuels. *Energy Fuels* **2012**, *26*, 380−390.
(89) Oluwatosin, A. A.; Oluwatobiloba, Q. R.; Samuel, L. O. Physicochemical assessment, pyrolysis and thermal characterization of *Albizia zygia* tree sawdust. *Int. J. Nanotechnol. Nanomed.* **2022**, *7*, 91−99.
(90) Sulaiman, M. A.; Adetifa, B. O.; Adekomaya, S.; Lawal, N. S.; Adama, O. O. Experimental characterization of maize cob and stalk based pellets for energy use. *Eng. J.* **2019**, *23*, 117−128.
(91) Odusote, J. K.; Adeleke, A. A.; Lasode, O. A.; Malathi, M.; Paswan, D. Thermal and compositional properties of treated *Tectona grandis*. *Biomass Convers. Biorefin.* **2019**, *9*, 511−519.
(92) Guo, T.; Ma, N.; Pan, Y.; Bedane, A. H.; Xiao, H.; Eić, M.; Du, Y. Characteristics of CO_2 adsorption on biochar derived from biomass pyrolysis in molten salt. *Can. J. Chem. Eng.* **2018**, *96*, 2352−2360.
(93) Salim, R. M.; Asik, J.; Sarjadi, M. S. Chemical functional groups of extractives, cellulose and lignin extracted from native *Leucaena leucocephala* bark. *Wood Sci. Technol.* **2021**, *55*, 295−313.
(94) Feng, S.; Yuan, Z.; Leitch, M.; Shui, H.; Xu, C. Effects of bark extraction before liquefaction and liquid oil fractionation after liquefaction on bark-based phenol formaldehyde resoles. *Ind. Crops Prod.* **2016**, *84*, 330−336.
(95) Ikubanni, P. P.; Adeleke, A. A.; Agboola, O. O.; Adesina, O. S.; Nnodim, C. T.; Balogun, A. O.; Okonkwo, C. J.; Olawale, A. K. Characterization of some commercially available Nigerian coals as carbonaceous material for direct reduced iron production. *Mater. Today: Proc.* **2021**, *44*, 2849−2854.
(96) Mallick, D.; Sharma, P.; Bora, B. J.; Baruah, D.; Bhowmik, R.; Barbhuiya, S. A.; Balakrishnan, D. Mechanistic investigation of pyrolysis kinetics of water hyacinth for biofuel employing isoconversional method. *Sustainable Energy Technol. Assess.* **2023**, *57*, No. 103175.
(97) Öhman, M.; Nordin, A.; Skrifvars, B.; Backman, R.; Hupa, M. Bed Agglomeration characteristics during fluidized bed combustion of biomass fuels. *Energy Fuels* **2000**, *14*, 169−178.
(98) Adeleke, A. A.; Odusote, J. K.; Lasode, O. A.; Ikubanni, P. P.; Madhurai, M.; Paswan, D. Evaluation of thermal decomposition characteristics and kinetic parameters of melina wood. *Biofuels* **2022**, *13*, 117−123.
(99) El-Sayed, S. A.; Xiang, J. Pyrolysis characteristics and kinetic parameters determination of biomass fuel powders by differential thermal gravimetric analysis (TGA/DTG). *Energy Convers. Manage.* **2014**, *85*, 165−172.
(100) Demirbas, A.; Arin, G. An overview of biomass pyrolysis. *Energy Sources* **2002**, *24*, 471−482.
(101) Gaitán-Álvarez, J.; Moya, R.; Puente-Urbina, A.; Rodríguez-Zúñiga, A. Thermogravimetric, devolatilization rate, and differential scanning calorimetry analyses of biomass of tropical plantation species of Costa Rica torrefied at different temperatures and times. *Energies* **2018**, *11*, No. 696.
(102) Waters, C. L.; Janupala, R. R.; Mallinson, R. G.; Lobban, L. L. Staged thermal fractionation for segregation of lignin and cellulose pyrolysis products: An experimental study of residence time and temperature effects. *J. Anal. Appl. Pyrolysis* **2017**, *126*, 380−389.
(103) Nurazzi, N. M.; Asyraf, M. R. M.; Rayung, M.; Norrrahim, M. N. F.; Shazleen, S. S.; Rani, M. M. S.; Rafiqah, S. A.; Aisyah, H. A.; Radzi, M. H. M.; Sabaruddin, F. A.; Sapuan, S.; Zainudin, E. S.; Abdan, K. Thermogravimetric analysis properties of cellulosic natural fiber polymer composites: A review on influence of chemical treatments. *Polymers* **2021**, *13*, No. 2710.
(104) Brebu, M.; Vasil, C. Thermal degradation of lignin - A review. *Cellul. Chem. Technol.* **2010**, *44*, 353−363.
(105) Yao, F.; Wu, Q.; Lei, Y.; Guo, W.; Xu, Y. Thermal decomposition kinetics of natural fibers: Activation energy with dynamic thermogravimetric analysis. *Polym. Degrad. Stab.* **2008**, *93*, 90−98.
(106) Boukaous, N.; Abdelouahed, L.; Chikhi, M.; Mohabeer, C.; Meniai, A.; Taouk, B. Investigations on Mediterranean biomass pyrolysis ability by thermogravimetric analyses: thermal behaviour and sensitivity of kinetic parameters. *C. R. Chim.* **2020**, *23*, 623−634.
(107) Xing, P.; Mason, P. J. R.; Chilton, S.; Lloyd, S.; Jones, J. R.; Williams, A. M.; Nimmo, W.; Pourkashanian, M. A comparative assessment of biomass ash preparation methods using X-ray fluorescence and wet chemical analysis. *Fuel* **2016**, *182*, 161−165.
(108) Zając, G.; Szyszlak-Bargłowicz, J.; Gołębiowski, W.; Szczepanik, M. Chemical characteristics of biomass ashes. *Energies* **2018**, *11*, No. 2885.
(109) Jia, Y.; Li, Z.; Wang, Y.; Wang, X.; Lou, C.; Xiao, B.; Lim, M. Visualization of combustion phases of biomass particles: Effects of fuel properties. *ACS Omega* **2021**, *6*, 27702−27710.
(110) Kongto, P.; Palamanit, A.; Chaiprapat, S.; Tippayawong, N. Enhancing the fuel properties of rubberwood biomass by moving bed torrefaction process for further applications. *Renewable Energy* **2021**, *170*, 703−713.
(111) Singh, S.; Chakraborty, J. P.; Mondal, M. K. Torrefaction of woody biomass (Acacia nilotica): Investigation of fuel and flow properties to study its suitability as a good quality solid fuel. *Renewable Energy* **2020**, *153*, 711−724.
(112) Gamgoum, R.; Dutta, A.; Santos, R.; Chiang, Y. Hydrothermal conversion of neutral sulfite semi-chemical red liquor into hydrochar. *Energies* **2016**, *9* (6), No. 435.
(113) Saxby, J. D. Atomic HC ratios and the generation of oil from coals and kerogens. *Fuel* **1980**, *59*, 305−307.
(114) Benoit, R. G.; Belhadj, N.; Serinyel, Z.; Dagaut, P. On the similarities and differences between the products of oxidation of hydrocarbons under simulated atmospheric conditions and cool flames. *Atmos. Chem. Phys.* **2021**, *21*, 7845−7862.
(115) Baloch, H. A.; Nizamuddin, S.; Siddiqui, M. M.; Riaz, S.; Jatoi, A. S.; Dumbre, D. K.; Mubarak, N. M.; Srinivasan, M.; Griffin, G. Recent advances in production and upgrading of bio-oil from biomass: A critical overview. *J. Environ. Chem. Eng.* **2018**, *6*, 5101−5118.
(116) Janković, B. D.; Manić, N.; Radović, I. B.; Janković, M. M.; Rajačić, M. Model-free and model-based kinetics of the combustion process of low rank coals with high ash contents using TGA-DTG-DTA-MS and FTIR techniques. *Thermochim. Acta* **2019**, *679*, No. 178337.
(117) Chen, D.; Gao, A.; Cen, K.; Zhang, J.; Cao, X.; Ma, Z. Investigation of biomass torrefaction based on three major components: Hemicellulose, cellulose, and lignin. *Energy Convers. Manage.* **2018**, *169*, 228−237.

https://doi.org/10.1021/acsomega.3c05656
ACS Omega 2023, 8, 43771−43791